Published in final edited form as:
Phys Med Biol. ; 67(16): . doi:10.1088/1361-6560/ac838f.

Advances and potentials of optical surface imaging in radiotherapy

Guang Li, PhD
Department of Medical Physics, Memorial Sloan-Kettering Cancer Center, New York, NY 10065

Abstract

This article reviews the recent advancements and future potentials of optical surface imaging (OSI) in clinical applications as a four-dimensional (4D) imaging modality for surface-guided radiotherapy (SGRT), including OSI systems, clinical SGRT applications, and OSI-based clinical research.

The OSI is a non-ionizing radiation imaging modality, offering real-time 3D surface imaging with a large field of view (FOV), suitable for in-room interactive patient setup, and real-time motion monitoring at any couch rotations during radiotherapy. So far, most clinical SGRT applications have focused on treating superficial breast cancer or deep-seated brain cancer in rigid anatomy, because the skin surface can serve as tumor surrogates in these two clinical scenarios, and the procedures for breast treatments in free-breathing (FB) or at deep-inspiration breath-hold (DIBH) and cranial stereotactic radiosurgery (SRS) and radiotherapy (SRT) are well developed. When using the skin surface as a body-position surrogate, SGRT promises to replace the traditional tattoo/laser-based setup. However, this requires new SGRT procedures for all anatomical sites and new workflows from treatment simulation to delivery. SGRT studies in other anatomical sites have shown slightly higher accuracy and better performance than tattoo/laser-based setup. In addition, radiographical image-guided radiotherapy (IGRT) is still necessary, especially for stereotactic body radiotherapy (SBRT). To go beyond the external body surface and infer an internal tumor motion, recent studies have shown the clinical potential 65 of OSI-based spirometry to measure dynamic tidal volume as a tumor motion surrogate and Cherenkov surface imaging to guide and assess treatment delivery. As OSI provides complete datasets of body position, deformation, and motion, it offers an opportunity to replace fiducial-based optical tracking systems. After all, SGRT has great potential for further clinical applications.

In this review, the OSI technology, applications, and potentials are discussed since its first introduction to radiotherapy in 2005, including technical characterization, different commercial systems, and major clinical applications, including conventional SGRT on top of tattoo/laser-based alignment and new SGRT attempting to replace tattoo/laser-based setup. The clinical research for

---

Correspondence: Guang Li, Ph.D., Attending Physicist, Department of Medical Physics, Memorial Sloan-Kettering Cancer Center, 1275 York Avenue, New York, NY 10065, lig2@mskcc.org, Phone: 212-639-2891, Fax: 212-717-3258.

PACS:
treatment strategy in, 87.55.-x
Treatment planning, 87.55.D-
in medical imaging, 87.57.Q-
Respiration, 87.19.Wx
Cancer, 87.19.xj

OSI-based tumor tracking is reviewed, including OSI-based spirometry and OSI-guided tumor tracking models. After all, the ongoing clinical research has created more SGRT opportunities for clinical applications beyond the current scope.

Keywords

Optical surface imaging; Surface-guided radiation therapy; Patient setup; Patient motion management

I. Introduction

Three-dimensional (3D) optical surface imaging (OSI) has been developed and applied in medical and clinical fields for many years (Winder, et al. 2005; O’Connell, et al. 2015; Hoisak and Pawlicki 2018; Padilla, et al. 2019; Li, et al. 2020), and it has been increasingly used in the radiotherapy clinic as surface-guided radiotherapy (SGRT) to facilitate patient setup and motion monitoring for breast cancer treatment, including deep-inspiration breath-hold (DIBH) for heart sparing of left-sided breast patients, and for stereotactic radiosurgery (SRS) of brain tumors, such as cancer metastases to the brain. Recently, a new paradigm of tattoo-less SGRT patient setup in radiotherapy is emerging to replace the traditional tattoo/laser-based patient setup tactics and workflow (Jimenez, et al. 2019; Rigley, et al. 2020), and the trend is extending beyond the brain and breast to other anatomic sites to eliminate the need of skin tattoos as OSI systems have become increasingly available in radiotherapy clinics.

In radiation therapy, it is most important to reproduce the tumor position before and during treatment to match the simulation position, on which the radiation treatment plan is created. In treatment simulation, computed tomography (CT) is often used to provide a patient’s three-dimensional (3D) anatomy, which may be combined with positron emission tomography (PET) and/or magnetic resonance imaging (MRI) via image registration for better tumor visualization and delineation, and the radiation beams are optimized to give a full prescribed dose to the tumor while maximally sparing nearby organs at risk (OARs) (Li, et al. 2021b). At the beginning of treatment delivery, the patient must be positioned the same as that at the simulation using image guidance, such as cone-beam CT (CBCT), orthogonal radiographic image pair, or fluoroscopic imaging as x-ray image-guided radiotherapy (IGRT), using 2D/3D/4D MRI for MRI-guided radiotherapy (MRgRT), or using 3D/4D OSI for SGRT. By aligning the setup images to the planning CT, MR, or any derived images, the patient’s tumor position at treatment simulation can be reproduced for radiotherapy delivery as planned. Although OSI only provides the external surface images, it contains ample patient anatomic information to achieve a surface match with the external contour of the simulation CT image. However, as a patient’s surface image does not necessarily infer the internal tumor position, the SGRT setup may still require IGRT to verify and adjust the setup by aligning the internal tumor or tumor surrogate, especially for hypo-fraction stereotactic body radiotherapy (SBRT). Ideally, if the external-internal relationship is known, SGRT alone can be used to infer the tumor position at patient setup with a proper safety margin, such as a superficial lesion (breast cancer) or lesion in rigid anatomy (brain cancer). In other words, the region of interest (ROI) within the OSI's field of view (FOV) as the patient positioning surrogate can also become a tumor positioning surrogate when the external-internal relationship is known. As OSI offers non-ionization imaging with sub-millimeter (mm) detectability, real-time performance, availability at all couch angles, and the largest FOV among all clinical imaging modalities, its advantages have been explored in recent years, promising for further clinical applications (Bert, et al. 2005; Cervino, et al. 2009; Li, et al. 2011a; Li, et al. 2016b; Wiersma, et al. 2016; Zhang, et al. 2021).

During treatment, OSI can provide real-time guidance to monitor a patient's head motion in SRS treatment or breathing motion in breast DIBH treatment, so SGRT treatment accuracy can be ensured to target the tumor while sparing the OARs. An optical system utilizing a few light-emitting markers or passive light-reflectors, which can be considered a simplified version of OSI, has been applied with a statistical predictive model in the Cyberknife Synergy system (Accuray Inc., Sunnyvale, CA) to treat lung or liver cancer, which moves with patient's respiration, in conjunction of periodic x-ray imaging verification (Meeks, et al. 2005; Lyatskaya, et al. 2008). Although the marker-based optical system provides simplicity, OSI should be a better alternative for patient motion monitoring and motion management, because not only does it eliminate the foreign markers by using the native body surface as the motion surrogate, but also it provides a dense point array that covers the moving ROI with a much higher spatial resolution (Willoughby, et al. 2012; Hoisak and Pawlicki 2018), although the temporal resolution limited by the speed of 3D reconstruction needs improvement (Li, et al. 2015b; Li, et al. 2016b). To infer internal tumor motion, a predictive tumor motion model based on physical, biomechanical, statistical, or machine learning methods and fed by the real-time OSI data could be applied to predict the position of an internal tumor during treatment (Hughes, et al. 2009; Fassi, et al. 2015; Li, et al. 2015b; Zhao, et al. 2016; Kim, et al. 2021; Wikstrom, et al. 2021).

As the OSI-based clinical SGRT applications are substantially increasing in recent years, about one review paper per year has been published since 2018, covering various aspects of the clinical applications (Hoisak and Pawlicki 2018; Padilla, et al. 2019; Batista, et al. 2020; Freislederer, et al. 2020), including the American Associates of Medical Physicist (AAPM) task group 302 report (Al-Hallaq, et al. 2022). These reviews provided great coverages on practical OSI-based clinical applications of commercial OSI systems, features, and functionalities, and recommended clinical quality assurance (QA). However, other OSI aspects may not be covered adequately, including a comprehensive discussion on all OSI technologies, the transition from conventional SGRT to tattoo-less SGRT, and OSI-related fundamental research with the potential for new areas of clinical applications. Therefore, another review of all aspects of OSI-based SGRT should still be beneficial to the field.

In this review, we will first discuss various types of commercial OSI technologies and their characterization with pros and cons, followed by conventional SGRT clinical applications, which are proceeded with conventional tattoo/laser-based setup. Then, it discusses the emerging efforts to replace the tattoo/laser-based patient setups with OSI-based SGRT setup, which removes the need for tattoo/laser alignment, leading to a paradigm-changing approach in radiotherapy, as shown in Fig. 1. As all advents of SGRT are based on clinical research, similar to the IGRT and MRgRT developments and their clinical applications, recent OSI-based studies are reviewed and discussed, which allows us to peek at what may occur in the future clinic. Finally, we will wrap up this review article with a summary and outlook.

II. The technology of Optical Surface Imaging (OSI)

A 3D surface image of a subject can be reconstructed based on the stereoscopic mechanism, similar to how human vision recognizes 3D objects. The same mechanism is used in marker-based detection, as a special case of the OSI, where only a few points (emitting or reflecting markers) on the patient's body surface as surrogates are measured. However, OSI is a better alternative, a marker-less tool for patient setup and motion monitoring in the radiotherapy clinic. This review article focuses on the structured-light OSI technique, its clinical research, and its clinical applications.

To help the 2 cameras to identify the same point in their views, the so-called structured light method is used to project a speckle light with a texture pattern on a patient body surface. Many points in the texture can be detected and uniquely identified by the 2 cameras in a camera pod with slightly different viewing angles. A triangle is formed among the two cameras and a point of interest and used to calculate the point location for the reconstruction of 3D surface images. Because of the high framerate of video cameras, the structured light method has the capacity of capturing real-time surface images (Wiersma, et al. 2016). Alternatively, a laser scanning and detecting system can also be applied to reconstruct 3D surface images from the triangle of the laser pointer, detector, and light spot on the surface. Compared with the structured light approach, however, the laser scanning method requires time to scan through the FOV, rather than an instant capture, therefore it is no longer used in the latest commercial system. Alternatively, fringe projection profilometry has also been developed for SGRT (Price, et al. 2012), using a pre-designed fringe pattern to decode the distorted pattern on the measurement object using Fourier transform filtering. Another OSI reconstruction method is the so-called time of flight (TOF) using a radiofrequency (RF) modulated light source (e.g., 30MHz) and detector to emit and detect the phase difference between the emitted and reflected lights, respectively, so the locations of a spot array can be calculated. This TOF camera is relatively inexpensive but has limited spatial resolution and detection accuracy (<5mm) (Wentz, et al. 2012).

So far, 3 major commercial OSI systems used in radiotherapy employ the structured light approach to achieve both high spatial and high temporal resolutions, including the AlignRT system (VisionRT, Ltd, London, UK), Catalyst$^+$ system (C-RAD AB, Uppsala, Sweden), and IDENTIFY system (Varian Medical Systems, Inc., Palo Alto, CA), as shown in Fig. 2. Other types of OSI techniques are also jointly used, such as the TOF imaging to detect the accessory in IDENTIFY system (Varian) and infrared (IR) imaging in the ExacTrac Dynamic system (BrainLab AG, Munich, Germany).

II.a. Stereoscopic imaging with discrete fiducial markers

The determination of a marker's position in space via a stereoscopic view is through forming a triangle between the marker (or the spot of interest) and the two cameras.

The marker can be either an active light-emitting diode (LED) or a passive reflector, and charge-coupled device (CCD) cameras are often used to capture the image of markers. Through the law of sine in trigonometry, the distances from both cameras to the marker point can be calculated because the distance between the two cameras and the two angles between the two cameras and the marker are known (Waghorn 2020). In practice, these system parameters are obtained through calibration using a set of markers with known physical locations. Therefore, the physical location of the marker can be calculated in the room coordinate system. When three or more fiducial markers are used, the position and orientation of the point array can be determined. As the markers are placed directly or indirectly on a patient's body surface, they serve as a surrogate of the patient's position with both translational and rotational motions in real-time as the CCD video camera system provides a high frame rate (30 Hz or higher). Commercial marker-tracking optical systems include the Polaris Vega (Northern Digital Inc., Bakersfield, CA), which has 0.045 mm accuracy for a moving object at 40 cm/s (Fattori, et al. 2021). The real-time positioning management (RPM, Varian) system or respiratory gating for scanners (RGSC, Varian) is another example, which contains a small light-weighted box that has 2–4 light reflectors to place on the patient's chest or upper abdomen as a patient motion surrogate (Wiersma, et al. 2016; Shi, et al. 2017). The advantage of the marker-based system is its simplicity and real-time performance for motion monitoring. The major drawbacks of marker-based techniques are the uncertainties on the spot selection, reproducibility of marker placement, rigidity of a marker array, and potential motion difference between the marker and patient (Riboldi, et al. 2006).

II.b. Stereoscopic imaging with a scanning laser light

Under the stereoscopic approach, a system with a scanning laser and CCD camera has also been used in the earlier version of the Catalyst HD system (C-RAD). At any given time, the laser produces a spot (or a line) on a patient's body surface and the camera image it, forming the key triangle to determine the physical location of the spot (or points on the curved laser line). After scanning through the whole body, the 3D body surface image can be reconstructed. In this approach, the laser spots on the curved laser line along a patient's body replace fiducial markers, providing a uniquely identifiable point array. This system has been applied for patient setup after traditional setup and compared with CBCT, and the OSI setup has slightly higher accuracy and performance than the laser positioning setup (Brahme, et al. 2008; Carl, et al. 2018; Meyer, et al. 2020; Swinnen, et al. 2020). As this is a marker-less approach, it eliminates the uncertainty of marker placement. The laser scanner can also project setup parameters onto the patient body, helping therapists in the setup. However, this method requires a fast rate of laser scanning to cover the FOV, limiting the frame rate. Therefore, the new Catalyst HD+ system start to use the structured light method, which captures the entire surface image instantly independent of the size of the FOV.

II.c. Stereoscopic imaging with a structured light

When a point array of a patient's body surface is uniquely identifiable, the positions of the points can be determined based on the same method as discussed above. In the structured light approach, the unique point array is created by a red/blue light with a texture pattern projected from a speckle projector, and 2 slightly different images are captured by the stereoscopic cameras in the pod. When the position of each point in the texture is determined, a 3D surface image is thus reconstructed. The structured light approach is also called active OSI, useful for feature-less flat surfaces, such as the skin, to create surface textures (Hoisak, et al. 2020), while utilizing native object features, such as edges and textures (Catherwood, et al. 2011), is a passive approach, such as the native Kinect (Microsoft), an inexpensive solution (Padilla, et al. 2015; Silverstein and Snyder 2017). The major commercial OSI are all active systems that have 3 ceiling-mounted camera pods in a radiotherapy room: one is in the front of the couch and two are on the lateral sides, as shown in Fig. 2. Using the isocenter as the reference, the 3 partial surface images reconstructed from data taken by 3 ceiling-mounted camera pods can be sutured up into one more complete surface image of a patient. To use an OSI system in the clinic, it must be calibrated and commissioned based on the potential uses in a local clinic after the acceptance test by an engineer from the OSI vendor (Willoughby, et al. 2012; Zhang, et al. 2021).

II.d. Calibration of a structured-light OSI system

The OSI system must be calibrated with known surface geometry. For example, the AlignRT system is calibrated using a flat white plate with a 32×32 (=1024) block dot array centered with a crosshair, which is aligned with the isocenter of the megavoltage (MV) linear accelerator (Li 2020; Zhang, et al. 2021). The flat calibration plate provides a 2D array of circular black dots with known geometric positions relative to the center of the plate, which is aligned to the Linac isocenter, so the plate calibration allows 3D surface reconstruction and determines the isocenter. The third dimension (vertical) has also been introduced via an additional raised-plate calibration (10cm above the vertical isocenter) or the advanced camera optimization (ACO) modeling with built-in 3D information (provided at installation and updated in annual maintenance services). Clinically, the 3D calibration reduces the so-called couch-angle-dependency error (Paxton, et al. 2017; Li 2020; Zhang, et al. 2021), and consequently reduces the false positives of patient head motion at a large couch rotation during brain SRS/SRT treatments (Li, et al. 2020). A monthly calibration is recommended by the vendor and daily QA is required before clinical use. It is worthwhile to note that the AlignRT daily QA is to check the integrity of the 3 ceiling-mounted camera pods, rather than to confirm system calibration accuracy.

For clinical SRS applications, it is recommended to further verify the isocenter accuracy using a cube phantom (15×15×15 cm^3), which contains 5 internal ball-bearing fiducials for MV imaging so the AlignRT isocenter can be aligned to the MV isocenter. The misalignment of the optical and MV isocenters can be corrected further reducing the couch-angle-dependency error. Note that the Linac couch walk (couch rotates away from the isocenter) is present within 0.5mm and is not corrected. As the active structured-light approach can capture the images with speckle patterns at high spatial and temporal resolutions, all 3 major commercial OSI systems (Fig. 2) utilize this active OSI approach. However, as the reconstruction of 3D surface images requires high computing power, the frame rate may be limited, especially for a large FOV at high spatial resolution.

II.e. An example of commercial OSI systems: AlignRT by VisionRT

In radiotherapy clinics, an SGRT setup is achieved by capturing an on-site treatment surface image and aligning it to the external body contour of the planning CT image as the reference OSI image. This has not been changed although AlignRT has gone through multiple major upgrades since 2005 (Bert, et al. 2005; Waghorn 2020). The latest system (version 6.3) is built based on a client-server architecture (Zhang, et al. 2021). All patient data are saved in a network SQL database server and updated/retrieved by local client systems through a mid-tier application server so that it is now in compliance with the US patient privacy regulation. In our institution, the AlignRT server system supports 24 AlignRT clients, including 20 online systems for patient treatment and 4 offline workstations for patient preparation. The system offers both static and dynamic image captures and performs automatic surface registration to the ROI defined on the DICOM (Digital Communication in Medicine) reference image. In the dynamic mode, Real-Time Delta (RTD), the framerate can be as high as 8–16 Hz for patient motion monitoring during breast DIBH and brain SRS treatments.

The local computer workstation that controls the OSI system usually has two sets of user interface devices (a monitor, keyboard, and mouse): one set is inside the room and the other is in the treatment console area. A hand-held remote-control device may also be available to allow therapists to capture images anywhere inside the room and a respiratory coaching monitor to allow a patient to control their breath-hold, facilitating in-room SGRT patient setup and outroom SGRT motion monitoring during treatment.

In addition to basic 3D/4D OSI functionalities, it is worthwhile to mention 3 new features: (1) Postural Video, which outlines major body structures from the reference image in the camera views to facilitate SGRT patient setup, (2) 3D Photo, which maps a high-resolution photo picture of a patient to the 3D surface to show details, and (3) Deformation, which displays 2 matched surface images in color-coded visualization of local surface differences between the reference and verification images. The Postural Video provides the RTD from three camera views in the entire FOV beyond the ROI, so the body outline can be used to guide the alignment of the arm and chin in real-time during breast patient setup to minimize breast tissue deformation and reproduce the positions of the breast and local lymph nodes (Li, et al. 2021a). The Deformation has a 2mm color variation scale by default to show where and how much the 2 surfaces are differed within the ROI, allowing therapists to see where deformation occurs and monitor the change of superficial lesions during multi-fraction radiotherapy treatments.

II.f. Fringe projection profilometry for 3D surface imaging

The fringe projection profilometry is an OSI system, in which a projector illuminates objects with a pre-designed pattern, such as a single, monochromic, and continuous sinusoidal fringe pattern, and a camera captures the pattern that is distorted by the object's surface (Price, et al. 2012). The fringe analysis utilizes Fourier transform to analyze the spatial phase difference embedded in the distorted fringe pattern of the image between the object position level from a flat reference level to convert the phase signal to 3D geometry (Feng, et al. 2021). The system calibration is critical to reliably and accurately reconstructing the 3D surface image. The spatial accuracy is within <2mm (90%) with real-time performance. So far, no vender has made this technology commercialized, limiting its clinical applications. The fringe projection can also be used as structured light to gain a surface texture for 3D surface reconstruction.

II.g. Stereoscopic imaging using the time-of-flight (TOF) mechanism

Another physical mechanism to measure a spot position on a 3D surface is the so-called TOF technique (Placht, et al. 2012; Wentz, et al. 2012). In this approach, the emitting light intensity is modulated with a high RF frequency, such as 30MHz, and the reflecting light from a surface reaches the detector with a relative phase difference. Based on the phase shift and light speed, the distance of light traveling can be calculated and therefore the location of the spot. Once an array of such spots is detected, the 3D surface image (such as 176×144 pixels) of the surface is then reconstructed. The TOF camera system is fast, small, and inexpensive, and therefore used heavily in computer vision where high spatial resolution is not required. In radiotherapy, the TOF camera is used as the 4th camera in the IDENTIFY system (Varian) to check the bar codes of treatment accessories and their physical locations. However, the TOF camera cannot be used for patient SGRT due to the following two major limitations: (1) the spatial resolution is limited to 2–5mm, and (2) the distance between the light source and the surface should cause a shift less than half of the period of the RF modulated light, usually less than 5 meters.

II.h. Superficial imaging using IR thermal signals from patients

Different from visible light, IR light has a certain penetration ability, especially at far IR frequency, therefore IR emission/reflection at or slightly below the skin can be detected. In radiotherapy clinics, an IR imager has been used in detecting reflecting markers for decades, such as the RPM system (Varian). But IR imaging of patients' anatomy is a recent development and application in radiotherapy clinics to provide a thermal image of the patient's body or map the superficial blood vessels under the skin of a patient's palm. In the Varian's IDENTIFY system, a palm reader applies IR light to read a patient's vein image under the skin with high resolution to quick check the patient's identity (ID) throughout radiotherapy simulation and treatment.

In the ExacTack Dynamic system (BrainLab), the single-camera pod contains a third IR camera, providing thermal images of a patient's body, which are co-registered with the 3D OSI images. So, by combining the optical surface image, IR thermal image, and x-ray images, ExacTrac Dynamic aligns and checks patient position with sufficient accuracy for radiotherapy treatment. An IR light (850nm) has been used as a nonvisible structured light for head motion tracking with 0.24mm and 0.1° accuracy (Olesen, et al. 2012). Using IR time-multiplexed structured light and triangulation, another OSI system aiming to image a patient's forehead for cranial SRS was reported (Wagner, et al. 2014). It is intended to compensate for the thickness of the soft tissue to align to the rigid skull structure for higher accuracy of skull registration. The special structured light was based on IR laser scanning to establish spatial correspondence even with partial viewing to triangulate the laser source, spot array, and imaging camera. This study suggests an opportunity to avoid soft-tissue deformation in SGRT applications.

II.i. Superficial imaging using Cherenkov radiation from treatment

Cherenkov emission is a blue light, produced by high-energy charge-carrying particles that travel through transparent dielectric media, such as water or air, faster than that of light in that media. When treating superficial lesions, such as breast cancer, Cherenkov emission from the radiation can pass through superficial tissue and Cherenkov imaging has been developed to visualize the radiated field and estimate radiation dose (Glaser, et al. 2012; Andreozzi, et al. 2015). As the Linac high-intensity radiation beam is pulsed with 5μs duration with a 5ms gap, gated-acquisition of the Cherenkov signal is applied, allowing the detection in the presence of ambient room light during treatment. An optical fiber sensor is used to detect radiation pulses to control the shutter of the CCD camera to synchronize the Cherenkov imaging. Under clinical conditions, this imaging technique has been studied to visualize the radiation field with the patient's surface anatomy (Jarvis, et al. 2014), estimate radiation dose (Bruza, et al. 2017), and study radiation biology (Glaser, et al. 2015).

Recently, the Cherenkov imaging system has been tested in clinical trials for both real-time patient motion monitoring during treatment and retrospective treatment assessment, including breast cancer and sarcoma, such as total skin electron radiation (Jarvis, et al. 2021). The real-time Cherenkov imaging application has helped to detect 6 minor events out of 64 treatments and allows online correction according to the plans. Cherenkov imaging can also be used to allow measuring accumulative radiation dose and retrospective analysis. As Cherenkov imaging utilizes superficial signal, it can only be applied in superficial treatment sites. Although we only briefly discussed this superficial imaging method, it has the potential for clinical applications as it detects and visualizes the radiation field and dose directly, including a hybrid approach with the 3D/4D OSI techniques. As Cherenkov imaging will be integrated with the AlignRT system, called DoseRT (VisionRT), becoming commercially available, and the clinical applications are expected to be substantially increased.

III. Conventional OSI-based SGRT Applications in Radiotherapy

The first two OSI studies for radiotherapy applications were reported in 2005 by two clinical research groups. One from the Massachusetts General Hospital (MGH) studied breast phantom to evaluate the early version of the AlignRT system in a clinical setting (Bert, et al. 2005). The spatial accuracy, temporal frame rate, and system stability were evaluated. The other group from Johns Hopkins University conducted another breast phantom study using a different OSI system (Djajaputra and Li 2005). After these feasibility studies, clinical investigations followed, and the OSI-guided radiotherapy procedures have been named surface-guided radiotherapy, or SGRT (Li, et al. 2012). To guide a patient's setup, an ROI is always drawn at the treatment site for patient alignment to the DICOM reference surface that is obtained from the external body contour of the simulation CT image, while the large FOV would be useful to align associated anatomy that affects the treatment site, such as the arm and chin in breast treatment, as shown in Fig. 3B.

III.a. SGRT for breast patient setup and treatment

Breast SGRT setup in free-breathing (FB).—In 2006, the MGH group conducted the first clinical study using an OSI system to assist patient setup for accelerated partial breast irradiation (APBI) (Bert, et al. 2006). The patient's body contour from simulation CT in DICOM format was used as the setup reference image. The accuracy of the OSI setup was assessed in 9 patients using the room laser and portal imaging data as references. In addition, the study also assessed the variations of the ipsilateral arm at the patient daily setups, which led to the development and implementation of so-called 2-step breast setup procedure (aligning the arm and chin first and then the breast) at the Memorial Sloan Kettering Cancer Center (MSKCC) since 2012 (Ho, et al. 2013; Ho, et al. 2019). Also in 2006, an Italian group reported their clinical investigation of 9 breast patients and compared the OSI setup with that using 10 optical fiducials (Spadea, et al. 2006). Due to tissue deformation, the OSI accuracy may vary with $\sigma = \pm 3$mm uncertainty on average for breast patients. Later studies also illustrated the uncertainty and variation in SGRT APBI patient setup (Gierga, et al. 2008; Riboldi, et al. 2009; Zhao, et al. 2019).

The OSI has been applied for setting up locally advanced breast patients with verifications using laser, portal film, orthogonal 2D kilovoltage (2DkV) radiograph, and CBCT (Ho, et al. 2013; Kuo, et al. 2019). As the targets include both the breast and local lymph nodes, IMRT or VMAT techniques have been used clinically (Ho, et al. 2019). A 2-step breast setup procedure has been established at MSKCC by first aligning a patient's arm and chin and then aligning the breast ROI (Fig. 3B) so that the anatomy of the breast can be better reproduced with minimal deformation and surrounding lymph nodes can be set up accurately without large displacement from the simulation (Li, et al. 2021a), as shown in Fig. 4. Only can OSI be applied to guide the 2-step in-room breast setup as it has a large FOV and real-time performance without radiation, useful for both APBI and VMAT breast setup and treatments. For APBI patient setup, 2DkV matching on surgical clips is still the clinical standard of care (Zhao, et al. 2019), and for VMAT breast setup, 2DkV verification may still be needed (Cravo Sa, et al. 2018; Hattel, et al. 2019), especially for large patients who may experience large daily variation due to breast deformation. The long-term pulmonary outcome of locally advanced breast IMRT treatments has shown a remarkably low rate of grade 3 toxicity in 113 treated patients, despite large planning tumor volume (PTV), including the breast/chest wall and regional nodes, such as internal mammary node (Ho, et al. 2019), as shown in Fig. 4.

SGRT for breast DIBH treatment.—The DIBH technique was first studied and applied for treating lung cancer as it significantly increases lung volume so more lung tissue can be spared (Mah, et al. 2000; Mageras and Yorke 2004). As heart toxicity became known from breast cancer radiotherapy (Adams, et al. 2003; Theodoulou and Seidman 2003), the DIBH technique has been applied to treat left-sided breast cancer. The DIBH monitoring technique was based on the RPM technique initially and has been changed to OSI-based techniques gradually (Cervino, et al. 2009; Tang, et al. 2014; Tanguturi, et al. 2015). Several comparison studies were reported to validate the SGRT DIBH setups using either orthogonal 2DkV radiographic imaging or CBCT, suggesting the possibility of using the OSI alone without tattoos (Jimenez, et al. 2019; Rigley, et al. 2020). However, it should be cautious to use SGRT to replace IGRT radiographic setup (Kuo, et al. 2019; Laaksomaa, et al. 2019). Conceptually, the body surface can serve as the patient positioning surrogate, but SGRT may not be used for final setup except when it can also serve as the tumor surrogate, such as superficial lesion of breast cancer.

For DIBH treatments, both DIBH and free-breathing (FB) CT images are often acquired so that there will be ample time for an initial 2-step breast setup in FB to align the arm and chin first (Li, et al. 2021a), which is important reproduce the simulation position and minimize the deformation of the breast and regional lymph nodes for targeting (Fig. 4), as even a small shift in the node positions from FB to DIBH could lead to delivered dose differences (Pazos, et al. 2019). In addition, the depth of breath-hold can be quantified between FB and DIBH body contours as DICOM references, particularly in the vertical direction, which is the surrogate of the separation between the heart and chest wall. After the FB setup, patients are audibly coached or visually guided to reproduce the DIBH position, which can be modified based on internal bony alignment, if 2DkV is prescribed. Therefore, both breast and lymph node positions are better reproduced and thus dosimetrically covered (Ho, et al. 2019; Li, et al. 2021a).

When a bolus is prescribed for breast DIBH treatment, a new OSI reference image must be acquired after the bolus is placed on a patient for treatment motion monitoring. Often a sticky bolus is used, which has a sticky inner surface attached to the patient's skin and a white-cloth-covered external surface for OSI image capture. When no bolus is used, we highly recommend still taking a new reference image, not only for the uniformity of clinical workflow but also for the simplicity of clinical operation, as the new reference resets the residual setup errors to null and only motion shifts from FB to DIBH are monitored. When the motion management interface (MMI) is enabled with a Linac system, the radiation beam can be held automatically if the motion goes out of ±3mm tolerance (Li, et al. 2021a). Occasionally, a patient could move her body away from the initial setup position and appropriate action should be taken, including redoing the FB/DIBH setup.

III.b. SGRT for intracranial SRS and SRT

In a traditional brain SRS treatment, a patient's head was immobilized on the treatment couch by drilling 4 surgical screws into the skull to hold a metal ring on the head as the localization and fixation system. Initial efforts to replace this invasive SRS procedure were to use a regular head immobilization device but set up with CBCT and monitor the patient's head motion in real-time by placing 5 LED markers on the head (Kai, et al. 1998) or 4–6 reflective markers on a mouth-bite frame to determine head's motion in six degrees of freedom (DOF) (Kamath, et al. 2005). The marker-based optical system is subject to marker placement variations, marker mobility relative to the patient's head, and/or the requirement of the patient's compliance to bite on the mouthpiece with uniform strength throughout the treatment.

To overcome these shortcomings, OSI was introduced to monitor patients' motion directly as the superior alternative. A volunteer study was conducted by the University of California at San Diego (UCSD) using only a customized headrest for head immobilization while monitoring head motion using AlignRT in this marker-less and mask-less approach

(Cervino, et al. 2010). However, as there is no restriction in the anterior and inferior directions, subjects can move out of tolerance, especially when they fall asleep (Cervino, et al. 2012). Li et al from the MSKCC reported their first clinical SGRT SRS procedure using the PingPoint immobilization device (Aktina Medical, Congers, NY), which contains a customized headrest and a mouthpiece, restricting head motion in all six directions (Li, et al. 2011a). They monitored 11 frame-based SRS treatments and 13 frameless SRS and SRT treatment fractions using OSI motion monitoring and found similar distributions of head motion between the 2 patient groups. Later on, they developed an open-face mask (Li, et al. 2013) that is used in the Freedom system (CDR Systems, Alberta, Canada) with both customized headrest and open-face mask for SRS treatments (Li, et al. 2015a). The opening facial area is used as the ROI for initial SGRT setup and motion monitoring during SRS treatment, as shown in Fig. 3A. As the SGRT setup is quick and sufficiently accurate that only a single CBCT acquisition may be needed, which often shows shifts within 2mm from the SGRT setup (Lee, et al. 2021). Based on this observation, the SGRT SRS procedure has been applied to treat brain SRT patients in our institution with an accelerated workflow and a reduced safety margin from 3mm to 2mm (Li, et al. 2020).

In order to apply an SGRT cranial SRS procedure in a clinic, the OSI system requires to be specially calibrated and commissioned to meet the overall <1.0mm accuracy requirement for SRS treatment and routine QA processes to ensure the accuracy and reliability of an OSI system (Peng, et al. 2011; Zhou, et al. 2021). SRS requires a much tighter QA tolerance than any other SBRT and conventional treatments. As discussed in section II.d, if an AlignRT system is to be used for SRS treatment, it is recommended to calibrate it using not only the calibration plate but also the calibration cube to verify the AlignRT isocenter congruence with the Megavoltage (MV) treatment beam. Moreover, as non-coplanar beams or arcs are always used in SRS treatments, the so-called couch-angle-dependency error must be measured and minimized to within 1.0mm, so that the systematic uncertainty of an OSI can be built into the clinical action threshold (Zhang, et al. 2021). It is worthwhile to emphasize that the ceiling-mounted 3-camera-pod OSI system can be used at any couch angle, unlike the gantry-mounted imaging system, such as the onboard imager (OBI, Varian), which is restricted to use only at couch zero position due to the concern of gantry-couch collision. This OSI feature meets the SRS needs perfectly, as non-coplanar beams or arcs are always used in SRS treatments. However, the couch-angle-dependency error should be quantified and minimized in the OSI system commissioning process, if the OSI is to be used for frameless SGRT SRS (Zhang, et al. 2021). Note that the couch walk error, usually within 0.5mm (Jursinic, et al. 2022), is also a cause for the couch-angle dependency error. When an OSI system is used for specific clinical applications, such as SRS or proton therapy (Fattori, et al. 2020), all involved OSI clinical features should be tested and covered by the commissioning procedure.

III.c. SGRT for proton or particle radiotherapy

For proton or particle radiotherapy, beam penetration depth from the skin surface is critical for dose delivery in addition to the isocenter correctness, so SGRT setup has been investigated, for instance, to measure the nozzle-skin air gap and SSD using a home-growth OSI method for a proton system (Mevion Medical Systems Inc., Littleton, MA), so an accurate target depth can be confirmed based on OSI and CBCT at treatment (Wang, et al. 2019). For historical reasons, SGRT applications for proton therapy are lagging from photon therapy, similar to IGRT applications.

An early study from the MGH on 15 postmastectomy chest wall patients compared SGRT setup with IGRT setup using radiograph and found OSI guidance reduced the setup uncertainty to 1.5mm, half of the radiograph-only setup error (~3mm), and also reduced the setup time by 550 about half (Batin, et al. 2016). Therefore, when there is not much tissue deformation involved, OSI provides a more accurate and efficient patient setup without extra radiation to the patients. Another study of 28 breast patients found that IGRT can be substituted by SGRT for postmastectomy chest wall patients, while large variations of SGRT were observed for patients with native breasts or large implants (Batin, et al. 2018). For respiratory-gated proton therapy, an optical marker-based system is still used (Fattori, et al. 2020), as OSI-based techniques are still in development phases to infer internal tumor motion (Glide-Hurst, et al. 2011), and more studies will be discussed in the Clinical Research section. In proton therapy, as the beam-tumor conformality is higher it requires highly accurate tumor localization using IGRT and low system latency if motion monitoring is needed. Due to the different configurations between the proton gantry and photon gantry, the locations of ceiling-mounted lateral camera pods are moved toward the frontal position with oblique angles away from the proton gantry.

III.d. SGRT in bore-configured Linac systems

There are several bore-configured Linac systems, including the Halcyon/Ethos systems (φ=100cm, Varian), TomoTherapy system (φ=85cm, Accuray Inc., Sunnyvale, CA), and MR-integrated Linac, such as the UNITY system (φ=70cm, Elekta, Stockholm, Sweden) and the MRIDIAN system (φ=50cm, ViewRay Inc., Oakwood Village, Ohio). Only Halcyon/Ethos systems with a sufficiently large bore size can be equipped with one of the two commercial OSI systems for SGRT. One system is the AlignRT inBore system (v7.0), which has three conventional ceiling-mounted external camera pods, as usual, to align patients at the virtual isocenter outside the bore and two in-bore camera pods in a ring structure frame attached to the internal surface of the bore (Nguyen, et al. 2020). This inBore OSI system is placed outside of beam fields so it does not interfere with dose delivery, and it is thin enough in the lower part of the ring, so it does not interfere with the anti-collision safety guard. It has an overall 0.5mm accuracy concerning the virtual-to-true ISO transfer, vibration due to gantry rotation, and couch sagging due to patients’ weight. However, this system requires re-calibration when the Linac needs open-cover services, and the camera ring mount needs to be taken off. As the Linac cover (OSI mounting base) is supported by a spring system, it may cause a 0.5mm uncertainty for the inBore system higher than the conventional ceiling-mounted system. However, as the Linac does not allow couch rotation, so no SRS treatments can be performed and 0.5mm uncertainty is acceptable.

Varian’s IDENTIFY provides an external SGRT solution, in which there are two ceiling-mounted frontal camera pods with ±20° from the central line and a third ceiling-mounted camera pod at the back. This SGRT system provides the frontal, some lateral, and back views so should provide sufficient body surface for surface alignment. As the system also contains a fourth TOF camera for accessory checks, it may provide a different clinical workflow from the AlignRT solution. A non-commercial in-bore single-camera motion monitoring system using a Kinect camera with structured light was reported with a 4Hz frame rate (Delombaerde, et al. 2019) and applied in motion monitoring of patient's chest motion to measure baseline drifts during treatments (Delombaerde, et al. 2021). A couch-mounted camera system may also be used for patient motion monitoring during treatment.

III.e. Other clinical applications using OSI

In addition to the common OSI applications for SGRT patient setup and motion monitoring in the two major anatomic sites, OSI has been applied in other aspects of radiotherapy, including patient identity checking, treatment accessory checking, and patient-gantry collision checking before or during treatments (Hoisak and Pawlicki 2018; Al-Hallaq, et al. 2021).

For patient identification, the AlignRT system has added another FDA-approved component, called SafeRT (VisionRT), using a facial identification algorithm based on machine learning, similar to the latest biometric authentication systems built into some mobile devices. Using wall-mount cameras, a patient's photo can be taken before simulation and treatment, so that the patient's ID can be confirmed through facial recognition, in addition to traditional manual checks (Silverstein and Snyder 2017). The IDENTIFY system uses an IR palm reader without physical contact for automatic patient ID identification via matching of the patient-specific blood vessel network. With the automatic patient ID check, patient treatment safety is therefore enhanced in busy radiotherapy clinics.

The OSI system has also been used to perform an automatic check of treatment accessories, including patient immobilization devices, such as a headrest, facial or body mask, body mold, breast board, and leg rest, and radiation modification devices, such as bolus, compensator, or electron cutout. The IDENTIFY system uses a fourth TOF camera above the couch (Fig. 2) to check the bar-code ID and location of these accessories on the treatment couch. The AlignRT and Catalyst systems also contain a module to allow accessory checks before the patient setup in the clinic. These patient-safety features add value to enhance treatment accuracy.

Additionally, the OSI systems are capable of checking the potential collision between the gantry and the patient during treatment, as the geometry of the patient and radiation gantry is known at the setup (Padilla, et al. 2015). It is worthwhile to mention that the Cherenkov surface imaging technique is going to be commercialized by VisionRT as a new product named DoseRT in the future. So, clinical applications of Cherenkov imaging are expected to be increased substantially, including real-time monitoring radiation field relative to treated patient anatomy in real-time. Overall, because of the non-ionizing feature and real-time performance with a large FOV, the OSI technology offers many surface-guided functionalities to help and facilitate clinical operations and workflow (Brahme, et al. 2008; Sharma, et al. 2011; Hoisak and Pawlicki 2018; Padilla, et al. 2019; Freislederer, et al. 2020).

IV. Toward Tattoo-less SGRT Setup and Monitoring Paradigm

It has been a new trend to apply OSI for patient setup at most anatomical disease sites, as a better alternative to the tattoo/laser-based setup strategy. The difference between conventional SGRT (discussed above) and tattoo-less SGRT can be illustrated in Fig. 1. The conventional SGRT adds OSI-guided alignment on top of the laser-based patient setup, which appears the case in the majority of the clinical studies discussed in section II and many studies in this section as well. Therefore, the conventional SGRT has duplicated the efforts in patient setup by using both approaches. The tattoo-less SGRT, on the other hand, is a true independent initial step in patient setup, which has been utilized in some clinics, but not many true tattoo-less SGRT publications without tattoo/laser pre-setup can be found. From patients' viewpoint, tattoos are not desirable for various reasons (Jimenez, et al. 2019), including the permanent emotional reminder of what they have experienced while seeking a cure for the deadly disease. Therefore, eliminating the use of tattoos in patient radiotherapy setup will improve patient care.

Technically, completely replacing tattoos with OSI to establish tattoo-less SGRT requires two major pre-conditions: (1) the SGRT setup can be applied to most treatment sites, if not all, and (2) the setup accuracy and performance should be at least equivalent or better than that of tattoo/laser setup. An extra benefit of the tattoo-less SGRT procedure is to provide motion monitoring during treatment. Clinically, the ROI creation for various anatomical sites should be carefully evaluated as a good body position surrogate, which may need modifications at setup by therapists to cope with patient-specific tissue deformation. The establishment and implementation of tattoo-less SGRT will impact the clinic significantly, as the tattoo technique has been used since the beginning of radiotherapy, even in the IGRT era, and clinical staff has to be re-trained to adopt this paradigm-changing technology. The clinical workflow and procedure are subject to change from treatment simulation to delivery.

Like any other imaging modalities that have been applied in the radiotherapy clinic, clinical studies have been and should always be performed before clinical implementation. So far, the two major established SGRT applications in breast (superficial lesion in deformable anatomy) and brain (deep-seated lesion in rigid anatomy) treatments have followed the research-to-clinic path. Although a lot of clinical work is required to implement tattoo-less SGRT procedures, studies have demonstrated that SGRT setup accuracy and performance are sufficient to replace tattoo/laser-based setups (Rigley, et al. 2020; Lee, et al. 2021). So far, the tattoo-less SGRT approach has been used for breast patients (Jimenez, et al. 2019; Rigley, et al. 2020). For other disease sites, however, limited clinical studies may have resulted in a lack of widespread clinical applications. Site-specific issues and complexities are very different, including head and neck, thorax, abdomen, pelvis, and extremity. In general, the more deformable the site is the larger uncertainties for the SGRT setup, and the more uncertain the external-internal relationship, the higher demand to use IGRT for the final setup, targeting an internal tumor. As SGRT studies have covered different anatomical sites, it is necessary to publish these results to share within the radiotherapy community to pursue tattoo-less SGRT applications.

IV.a. SGRT setup for head-and-neck (HN) patients

In HN treatments, an early report from Duke University was to simulate OSI patient setup accuracy of 11 patients using 77 weekly CBCT external contours. As the CBCT dataset contains both external and internal anatomy, the study found that the further away a lesion from the skull the higher uncertainties were expected using an OSI-guided setup compared with radiographic imaging (Gopan and Wu 2012). This observation was confirmed by an OSI study of 60 HN patients that were sorted into 3 groups: the nasopharynx, oral cavity, and oropharynx under clinical conditions (Wei, et al. 2020). They found that SGRT setups were significantly better than conventional setups using skin markers, and the nasopharynx group has the least SGRT setup errors. For superficial neck lesions, a study compared optical scanning images from a hand-held scanner with MRI images and showed a strong correlation, illustrating the ability of tumor volume assessment based on surface imaging (Kim, et al. 2021).

For HN patient setup, an open-face mask was studied to help immobilize HN patients who suffer from mild claustrophobia to go through radiotherapy treatment (Li, et al. 2013). Recently, another prospective study reported a direct evaluation of AlignRT setup accuracy based on 269 patients in 415 SRS treatments (Lee, et al. 2021). An AlignRT verification image was captured after CBCT setup shifts at the treatment position so AlignRT shifts represent their differences, which show the mean vector errors of 1.0±2.5mm and −0.1±1.4° and the 95% confidence interval within 5mm and 3°. A few outliers were found for very posterior lesions and explained based on mild correlations between the longitudinal shift and pitch rotation and between the lateral shift and roll rotation, owing to surface registration uncertainty (or ambiguity) of the OSI that has a bias on the anterior surface ROI. Also, the initial SGRT patient setup before CBCT is fast with an average time of 0.8±0.3 mins. Therefore, an SGRT setup has better performance and higher accuracy than a traditional setup using room lasers, and is, therefore, suitable for conventional radiotherapy of whole or partial brain and nasopharynx cancer treatments.

In the neck region, it is still a clinical challenge to set up cervical spine (c-spine) curvature reproducibly, as it involves online patient adjustment and no effective radiographic imaging is available for setup guidance. The investigators at MSKCC have reported a novel approach to accurately setting up c-spine curvature by introducing two ROIs in SGRT and a movable head support allowing longitudinal shifts up to 3cm in a 10-volunteer experiment (Li, et al. 2016a). In this study, an ROI on the shoulder was first aligned, followed by a second ROI on the facial area of the open-face mask by adjusting the longitudinal position of the head within 3cm. The SGRT results were verified using lateral photography pictures to show both anterior and posterior neck outline curvatures. In contrast, as the single facial ROI does not cover the neck, so it is not a surrogate for the neck position and may only be applied to the sites near the skull (Wei, et al. 2020; Lee, et al. 2021) while the setup uncertainties are expected to be increased as the treatment site is further away from the skull (Gopan and Wu 2012).

IV.b. SGRT setup for thoracic patients

For the thoracic site, the most clinically relevant disease site is breast cancer, which was in fact the first site for SGRT setup. Schoffel et al conducted one of the earliest studies to assess the accuracy of the AlignRT system with 2 camera pods on an anthropomorphic body phantom and 4 healthy volunteers (Schoffel, et al. 2007). The accuracy was found to be 0.40±0.26mm in phantom and 1.02±0.51mm in volunteers, in reference to skin marker-based alignment. Gierga et al from MGH and Alderliesten et al from the Netherlands Cancer Institute (NKI) reported their clinical experience of SGRT setup for left-sided breast cancer patients (Gierga, et al. 2012; Alderliesten, et al. 2013b). As breast DIBH treatments require patients' participation, the DIBH reproducibility (Cervino, et al. 2009) and heart position variations (Alderliesten, et al. 2013a) are important factors in SGRT DIBH treatments. Even though only partial DIBH may be achieved by some patients in the clinic due to their inability to persistently perform DIBH as simulated, the heart dose can still be reduced substantially compared with FB setup and treatment (Wiant, et al. 2015).

In addition to the traditional whole breast treatment, accelerated partial breast irradiation, or APBI, is often used to treat early-stage breast cancer. The first clinical application was reported on a 9-patient APBI study using AlignRT from MGH (Bert, et al. 2006). The accuracy, or the distance of reference-to-verification surfaces, was reported to be 1.6±2.4mm on average in comparison with the portal film. It is worthwhile to mention that gated OSI was used in the APBI study to achieve a mean target registration error of 3.2mm from the first fraction reference (Gierga, et al. 2008). However, in terms of 6DOF shifts, Zhao et al from the University of Utah found 9 out of 12 APBI patients had ≥ 5mm maximum shifts, although 11 out of 12 had mean shifts of < 5mm, compared with IGRT setup using a CT on rail system (Zhao, et al. 2019). Jimenez et al from MGH have recently demonstrated that SGRT setup can provide slightly better accuracy, precision, and performance than tattoo/laser-based patient setup, and therefore, they concluded that SGRT can be used in the clinic to replace the tattoo/laser-based patient setup (Jimenez, et al. 2019). In APBI treatments, the margin required for tumor bed targeting is often 1.5–2.0 cm and fiducial-based radiographic imaging is still the standard of care in the clinic (Yang, et al. 2013), although the SGRT setup uncertainty may be tolerable.

From the CNS and HN to the thorax and abdomen, a recent study of 894 patient plans with 16,835 treatment fractions found that the uncertainty ranges increase from 2–3mm to 9–11mm for 90% of the cases (Haraldsson, et al. 2020). The Sentinel OSI system (C-RAD) was used and compared with MVCT from TomoTherapy (Accuray Inc.). The ranges of residual errors in the SGRT setup are significantly lower than the tattoo/marker-based setup for all 4 anatomical sites, as shown in Fig. 5. The close-to-zero mean residual error with a lower standard deviation of SGRT setup suggests that SGRT is capable of replacing tattoo/laser-based patient setup. As this study referenced the internal tumor, however, the large SGRT setup variation indicates that the external-internal relationship is uncertain and IGRT is still needed for thoracic and abdominal setup. This study is consistent with an earlier study of 110 patients with 1902 treatments (Carl, et al. 2018) and another study of 284 SBRT patients with and without surface guidance (Leong and Padilla 2019).

IV.c. SGRT setup for abdominal, pelvis, and extremity patients

With the DIBH technique developed initially to treat lung cancer and the recent success in SGRT DIBH for breast cancer, it is logical to apply the SGRT DIBH technique to treat lung and abdominal cancer. Recently, a study has reported the SGRT DIBH technique for hypo-fractional stereotactic body radiotherapy (SBRT) of 3 lung and 7 liver cancer patients as an effective tool for motion management (Naumann, et al. 2020). A major advantage of changing treatment from FB to DIBH is the PTV reduction from 145cc to 110cc. After the SGRT DIBH setup, the IGRT DIBH setup using CBCT yields significantly higher mean shifts in the liver (9mm) than in the lung (5mm). To monitor the abdominal motion, it is recommended to exclude the rib cage from the ROI (Fig. 3C) as the lower rib cage moves with the upper one, namely the thorax (Hughes, et al. 2009; Li, et al. 2015b; Li, et al. 2016b; Song, et al. 2022). The area of the abdominal surface with or without the support or restriction from the rib cage moves differently (further discussion in the clinical research section).

In the pelvis, only a few site-specific SGRT studies have been published, in contrast to other anatomic sites. As early as 2009, the SGRT setup for 16 prostate patients was studied to assess setup reproducibility (Krengli, et al. 2009) by comparing OSI alignment with the setup using the electronic portal imaging device (EPID). Using EPID references, another SGRT investigation of 19 prostate patients showed that ~45% of SGRT setups had beyond 5mm differences in vertical and longitudinal directions (Bartoncini, et al. 2012). A recent study compared the performance of SGRT setup with the conventional 3-point setup and found slightly better setup accuracy and speed (Mannerberg, et al. 2021). These studies are consistent with the results shown in Fig. 5. Therefore, SGRT seems ready to work alone for patient setup, while IGRT with radiographic imaging is still necessary as the body surface cannot serve as a tumor surrogate in this case.

For the extremity, SGRT has its advantage to help patient setup. Earlier on, optical reflection markers were tested for intrafractional motion after CBCT patient setup on 17 patients (Dickie, et al. 2010). An SGRT study of 16 patients over 236 treatments found an intrafractional motion of 2.1±1.3mm and interfactional correction of ~3–4mm in any direction (Gierga, et al. 2014). As the extremity lesions may be superficial, similar to some HN cases, the growth or shrinkage of the lesions after simulation or during treatment may affect the surface matching for SGRT setup, but OSI can help to detect the superficial changes.

After all, tissue deformation may appear to be a major obstacle for SGRT setup, although the tool to assess surface deformation is available, such as a color-coded deformation viewing tool in the AlignRT system. Clinically, how to handle tissue deformation in SGRT is still one of the most challenging questions, and the solution to address this challenge is through conducting site-specific SGRT studies to develop, implement and, support clinical SGRT.

V. Clinical Research and Future Applications

The two most important questions among many clinical challenges in OSI applications in radiotherapy clinics are (1) how to handle body deformation and (2) how to infer internal organ location and motion from the external body surface motion, as the solutions to these questions will lead to new clinical SGRT applications. Three early studies on two OSI-based respiratory surrogates (Hughes, et al. 2009) and the feasibility of OSI-based spirometry (Li, et al. 2009a; Li, et al. 2009b) were reported, demonstrating more potential OSI applications in the clinic.

V.a. OSI-based spirometry to measure respiratory tidal volume

To infer thoracic or abdominal tumor motion based on OSI data, volumetric approaches were reported to create ventilation surrogates. In 2009, two consecutive studies reported volumetric calculation of patients' respiratory tidal volumes and external-internal motion modeling based on 4DCT of the entire torso, suggesting that OSI could be used to measure respiratory tidal volume (Li, et al. 2009a; Li, et al. 2009b). Respiratory tidal volume has been studied as a good surrogate of tumor motion in lung and liver cancer (Keall, et al. 2006). In the same year, an independent study reported a volumetric and a fiducial-like ventilation surrogate based on OSI image data (Hughes, et al. 2009). They calculated volume differences under two body surfaces at different respiratory phases to infer respiratory motion. These studies initiated a new path to apply the moving and deforming OSI surface data for clinical applications, triggered the development of OSI-based spirometry (Li, et al. 2015b; Li, et al. 2016b) and predictive model using OSI data as input (Yuan, et al. 2016).

When the entire human torso is studied as a closed system, meaning that no materials go in and out of the system, it allows the basic physical laws to work, such as the mass conservation law and ideal gas law. With such a closed system, it was hypothesized that the amount of air that a patient breathes in and out is the cause for, and therefore should be equal to, the volume change of the torso, namely a measure of tidal volume if the reference surface is at the full exhalation. Based on 4DCT data, this hypothesis was tested to be valid (Li, et al. 2009a; Li, et al. 2009b). When using the AlignRT system with 3 ceiling-mounted camera pods, only anterior and lateral torso surface motions can be viewed when a patient lies in the supine position. Although the posterior body surface is not seen, it has little motion as it is supported by the couch. Therefore, the OSI data are sufficient to calculate torso volume change, as shown in Fig. 6. The validation of the OSI-based spirometry was performed on 11 healthy volunteers (six female volunteers wearing form-fitting leotards) in reference to concurrent measurement using a conventional spirometer (Li, et al. 2015b; Li, et al. 2016b). The results showed that the difference between the two spirometry measurements is −2.2% ±4.9% and the correlation coefficient is 0.98±0.01 over multiple cycles of respiration in FB (78±28 cycles per volunteer on average).

The OSI-based spirometry also works for different breathing patterns, including FB, belly breathing (using the diaphragm), and chest breathing (using the intercoastal muscles), as shown in Fig. 7, suggesting the versatility and robustness of this OSI-based technique. The feasibility study was based on the real-time raw imaging data, which were used to reconstruct 3D surfaces retrospectively for volume calculation.

The findings from this study were consistent with an earlier report (Cala, et al. 1996), in which 86 reflecting markers (42 anterior, 34 posterior, and 10 lateral) were used to capture torso surface motion at 100Hz and measure the tidal volumes of two standing subjects. The detected optical point positions were linked as a triangulated mesh to create the torso surface and then calculate the tidal volumes that highly correlate with spirometry measurement. Comparing the fiducial study and the OSI-based spirometry suggests that lowering spatial resolution OSI with a smaller dataset is an option to achieve real-time computation and assuming negligible posterior motion in the supine position is valid. As a volumetric motion surrogate tends to outperform a point-based surrogate to infer respiratory-induced tumor motion (Hoisak, et al. 2006; Werner, et al. 2010), the OSI-based spirometry offers an advantage over the marker-based motion tracking system due to its high accuracy and simplicity without marker placement.

To apply the OSI-based spirometry in radiotherapy clinics, the OSI system must be improved to provide real-time reconstructed 3D surface data at a higher frame rate, so that the tidal volume can be calculated and tumor motion can be predicted in real-time to guide clinical operations. To ensure that a patient can be seen regardless of the positions of the radiation gantry and imaging arms, it was suggested to modify the OSI as a 4-camera-pod system by splitting the frontal camera pod into two with ±20° from the couch zero position, so that the machine isocenter can always be in the camera views without the camera-view blocking problem (Li, et al. 2016b). In fact, this configuration has been adopted as part of the IDENTIFY configuration for the Halcyon or Ethos Linacs. Note that when intrafractional on-board kV imaging or MV/kV is prescribed, 860 the views of the lateral two camera pods are blocked at most gantry rotation angles, making SGRT motion monitoring impossible to perform. Then, a fiducial-based motion management device, such as the RPM, is needed. However, the suggestion of the 4-camera-pod OSI system should work as the two frontal camera pods can see the patient around the isocenter, similar to the IDENTIFY/Halcyon system. So, it is critical to have vendors' participation and support to improve the OSI-based techniques for potential SGRT applications.

V.b. Predicting internal organ motion based on OSI

As the OSI can provide the most comprehensive external torso motion information, ideally it should offer the best opportunity to establish an external-internal motion relationship, compared with marker-based point array or local surface surrogates. In other words, if an external-internal tumor motion predictive model can be developed for clinical use with sufficient accuracy and reliability, OSI should offer the best chance to achieve this objective. Based on the 4DCT and AlignRT studies (Li, et al. 2009a; Li, et al. 2009b; Li, et al. 2015b; Li, et al. 2016b), a physics-based respiratory motion perturbation (RMP) model was proposed and studied using 2 sets of 4DCT images at simulation and treatment in 10 lung patients (Yuan, et al. 2016). This RMP model predicts tumor motion variation from a baseline obtained from one 4DCT by quantifying the breathing condition variations using the other 4DCT, such as the variations in tidal volumes and their distributions between the thorax and abdomen, and applying an improved expandable piston model to predict lung motion (Li, et al. 2009b). The final motion prediction, which is the sum of the predicted motion variations and the motion baseline, improved the tumor positioning accuracy by ~40% from an average of 2.0±2.8mm (difference between 2 4DCTs) to 1.2±1.8mm, similar to an established 5D model (Low, et al. 2005). As discussed above, the respiratory tidal volume and its distribution between the thorax and abdomen are both measurable using OSI.

For proton therapy, tumor motion prediction may also need to cover the lung tissue density and the location of nearby OARs to calculate the water equivalent length along the beam path. Fassi et al developed a surrogate-driven deformable motion model for organ motion tracking in particle radiotherapy (Fassi, et al. 2015). To achieve a volumetric motion model, 2 sets of 4DCT were used to deform from one to another using deformable image registration (DIR) and adapt to any inter-fractional baseline variations. A respiratory surrogate signal was extracted from the external surface to obtain both amplitude and phase factors to account for intra-fractional motion variations. Seven lung cancer patients were recruited for this study and the overall geometrical and water-equivalent-length accuracy was within 2mm. Zhang et al. also reported a volumetric motion model using DIR with the principal component analysis (PCA) (Zhang, et al. 2007), which allows real-time motion prediction using a single radiographic image (Li, et al. 2011b) and may be applied for prediction using the OSI signal to feed the DIR-PCA model. Ernst et al. studied 304 respiratory motion traces with an average duration of 71 minutes and extracted 21 features (12 from the time domain and 9 from the frequency domain) (Ernst, et al. 2011). Using three regression-based algorithms with major 6 features out of 21, the authors demonstrated that high motion prediction reliability can be identified through classification before treatment. So, for patients with high reliability of motion prediction, they can be selected to be beneficial from motion-compensated radiotherapy treatment, such as respiratory gating or tumor tracking.

A better motion ground truth with both internal and external data would be time-resolved 4DMRI, which has been recently developed using super-resolution image reconstruction to provide continuous external and internal organ motions over multiple breathing cycles (Li, et al. 2017; Li, et al. 2018; Nie, et al. 2020). Such datasets can be used as the ground truth to develop, improve, and validate motion prediction models. In addition to physical approaches (Low, et al. 2005; Yuan, et al. 2016), statistical and machine learning approaches were applied to establish the external-internal motion relationship (Hughes, et al. 2009; Li, et al. 2015c; Milewski, et al. 2019). As more patients' TR-4DMRI image data become available, a deep learning approach can also be applied.

A just-in-time prediction for about 500ms ahead of anticipated motion has been studied using a temporal convolutional neural network to overcome the system latency in motion tracking for Cyberknife Synchrony (Accuray Inc.) (Chang, et al. 2021). It is worthwhile to mention that the Cyberknife motion model is based on fiducial markers, which simplify external motion and reduce the computation time. A study has shown that the optical motion monitoring system is superior to the electromagnetic tracking system for its robustness and accuracy (Fattori, et al. 2017). An OSI-based motion prediction requires a more sophisticated approach to handle more comprehensive motion data, and therefore, potentially it could provide a better clinical solution in light of the booming of deep learning technology.

After all, by applying the OSI-based spirometry technique to feed and update an external-internal motion predictive model, it is promising to establish an accurate and reliable clinical system for patient motion monitoring with periodic x-ray verification during treatment using a conventional Linac, given the limited patient access to an MR-integrated Linac.

V.c. Improvements and promises of OSI for future clinical applications

The major issues that need to address for any OSI system include the real-time performance to reconstruct 3D surface images with a large FOV and the elimination of gantry blocking during IMRT/VMAT treatment delivery. Real-time performance is required for motion management, including image capturing, 3D surface reconstruction, and post-imaging computation for tumor motion prediction. Currently, only a fiducial-based optical system can provide real-time motion tracking. With the parallel computing technology using GPU (graphic processing unit), it is feasible but needs efforts from the OSI vendors. For the 3-camera-pod OSI configuration in a treatment room, some part of the patient body surface (>50% ROI) may be blocked by the MV gantry, EPID panel, or kV arms, especially when the IMR (intrafraction motion review) imaging or MV/kV imaging is required during SBRT treatments. Currently, the clinical solution is to use the RPM system instead of OSI, so that it allows treatment with both optical marker and x-ray imaging for intrafractional motion monitoring. As discussed above, a 4-camera-pod system can resolve this clinical issue by splitting the central (frontal) camera pod into 2 frontal camera pods with ±20° around the original central position. Therefore, the patient body surface around the isocenter is always visible throughout the treatment, useful for both current clinical procedures and future development of an OSI-based motion tracking system.

It is worthwhile to mention that tattoo-less SGRT setup is different from IGRT setup, as the OSI is simply replacing tattoos but not IGRT. Conceptually, as OSI can serve as a body position surrogate it can replace the tattoo; however, if OSI can also serve as a tumor surrogate, SGRT may be used alone with an appropriate margin for setups, such as SGRT setup for conventional treatment of brain and nasopharynx cancer (Lee, et al. 2021). When implementing a tattoo-less SGRT procedure in a clinic, it simply replaces the tattoos but not IGRT. Any IGRT requirement used currently should still be applied. For SBRT treatments, IGRT should always be applied to provide an accurate target position. Only when the external-internal relationship is known, then SGRT may be applied alone for conventional treatments.

Looking forward, three of the most challenging questions in clinical SGRT, although have been tackled, remain to be addressed: (1) automating ROI selection and creation for different anatomical sites, (2) handling tissue deformation within ROI, and (3) inferring internal tumor position and motion. The selection of a reliable ROI is important for any anatomical site and affects setup accuracy, and therefore, needs to be carefully studied and then implemented in routine clinical practice with automation. To establish the tattoo-less SGRT procedures for all anatomical sites, tremendous efforts for clinical research and implementation are required to study, validate, and optimize reliable ROIs and new clinical procedures and workflows without permanent skin marks from treatment simulation to delivery. More clinical tools are needed to represent, visualize, and quantify tissue deformation to facilitate clinical operations with more suitable, intellectual guidance. Applying IR laser scanning to retrieve bony surfaces under a thin layer of soft tissue may be a feasible approach to avoid deformation uncertainty in tracking patient motion. So far, no OSI-based motion tracking system is available in the clinic, although OSI offers the most complete external motion information and thus the best opportunity to fill the clinical need and improve the current practice. Combining the advents in medical imaging, such as time-resolved 4DMRI and deep learning strategy to train and validate more accurate and robust tumor motion prediction models, more OSI-based techniques can be further developed and applied for SGRT to guide motion-compensated radiotherapy in the future.

As the need for rapid daily planning and plan adaptation has increased, these treatments can be also accelerated using OSI guidance, especially the tattoo-less SGRT for most anatomic sites. In MR-integrated Linac systems, if an OSI system is available in the room, it should be useful to achieve body alignment and minimize external body deformation in real-time outside of the bore, and then place the anterior coil on the bridge frame and send the patient into the bore for MR imaging, setup, and daily adaptive planning. Because the patient has optimally aligned with minimal external deformation, the isocenter shift can be minimized and the complexity of daily planning adaptation is likely to be reduced.

VI. Conclusion Remarks

This article has reviewed the latest commercial OSI systems, clinical SGRT applications, and clinical OSI research for SGRT patient setup and motion monitoring in radiotherapy treatment. Clinically, SGRT has the potential to replace tattoo/laser-based patient setup and this trend has started, addressing patients' concerns and facilitating clinical workflow with improved setup accuracy and performance. As OSI is a non-ionizing radiation imaging technology, it can be applied for in-room real-time patient setup and patient motion monitoring throughout the entire treatment. Unlike other clinical imaging modalities, OSI provides the largest field of view for patient setup, allowing for the alignment of associated body parts to minimize the deformation at the treatment site. As the tattoo/laser-based patient setup procedure has been established since the beginning of radiotherapy, its replacement using OSI for SGRT patient setup will introduce a significant change in clinical practice. When implementing SGRT setup procedures for new anatomic sites, additional clinical investigations, as well as technical guidance from AAPM (Al-Hallaq, et al. 2022), are helpful to address site-specific issues. SGRT setup, however, may still need IGRT for targeting internal tumors, especially for hypo-fractional SBRT. Only when the external-internal positioning relationship is known, such as superficial lesions or lesions in rigid anatomy, SGRT can be used alone to set up patients for conventional radiotherapy treatment with an appropriate margin. For respiratory-induced tumor motion, the OSI-based spirometry offers the most comprehensive external motion dataset, including dynamic tidal volume and its distribution to feed an external-internal motion model to infer tumor position in real-time with periodic radiographic verifications. With further clinical investigations, we believe more OSI-based technologies and SGRT procedures are on the horizon for future applications.

Acknowledgments:

This research is in part supported by the MSK Cancer Center Support Grant/Core Grant (P30 CA008748).

REFERENCES:

Adams MJ, Hardenbergh PH, Constine LS and Lipshultz SE, 2003. Radiation-associated cardiovascular disease. Crit Rev Oncol Hematol 45:55–75. [PubMed: 12482572]

Al-Hallaq H, Batista V, Kugele M, Ford E, Viscariello N. and Meyer J, 2021. The role of surface-guided radiation therapy for improving patient safety. Radiother Oncol 163:229–236. [PubMed: 34453955]

Al-Hallaq HA, Cervino L, Gutierrez AN, Havnen-Smith A, Higgins SA, Kugele M, Padilla L, Pawlicki T, Remmes N, Smith K, Tang X. and Tome WA, 2022. AAPM task group report 302: Surface-guided radiotherapy. Med Phys 10.1002/mp.15532.

Alderliesten T, Betgen A, Elkhuizen PH, van Vliet-Vroegindeweij C. and Remeijer P, 2013a. Estimation of heart-position variability in 3D-surface-image-guided deep-inspiration breath-hold radiation therapy for left-sided breast cancer. Radiother Oncol 109:442–447. [PubMed: 24161569]

Alderliesten T, Sonke JJ, Betgen A, Honnef J, van Vliet-Vroegindeweij C. and Remeijer P, 2013b. Accuracy evaluation of a 3-dimensional surface imaging system for guidance in deep-inspiration breath-hold radiation therapy. Int J Radiat Oncol Biol Phys 85:536–542. [PubMed: 22652107]

Andreozzi JM, Zhang R, Glaser AK, Jarvis LA, Pogue BW and Gladstone DJ, 2015. Camera selection for real-time in vivo radiation treatment verification systems using Cherenkov imaging. Med Phys 42:994–1004. [PubMed: 25652512]

Bartoncini S, Fiandra C, Ruo Redda MG, Allis S, Munoz F. and Ricardi U, 2012. Target registration errors with surface imaging system in conformal radiotherapy for prostate cancer: study on 19 patients. La Radiologia medica 117:1419–1428. [PubMed: 22580804]

Batin E, Depauw N, Jimenez RB, MacDonald S. and Lu HM, 2018. Reducing X-ray imaging for proton postmastectomy chest wall patients. Pract Radiat Oncol 8:e266–e274. [PubMed: 29907510]

Batin E, Depauw N, MacDonald S. and Lu HM, 2016. Can surface imaging improve the patient setup for proton postmastectomy chest wall irradiation? Pract Radiat Oncol 6:e235–e241. [PubMed: 27025165]

Batista V, Meyer J, Kugele M. and Al-Hallaq H, 2020. Clinical paradigms and challenges in surface guided radiation therapy: Where do we go from here? Radiother Oncol 153:3442.

Bert C, Metheany KG, Doppke K. and Chen GT, 2005. A phantom evaluation of a stereovision surface imaging system for radiotherapy patient setup. Med Phys 32:2753–2762. [PubMed: 16266088]

Bert C, Metheany KG, Doppke KP, Taghian AG, Powell SN and Chen GT, 2006. Clinical experience with a 3D surface patient setup system for alignment of partial-breast irradiation patients. Int J Radiat Oncol Biol Phys 64:1265–1274. [PubMed: 16504764]

Brahme A, Nyman P. and Skatt B, 2008. 4D laser camera for accurate patient positioning, collision avoidance, image fusion and adaptive approaches during diagnostic and therapeutic procedures. Med Phys 35:1670–1681. [PubMed: 18561642]

Bruza P, Andreozzi JM, Gladstone DJ, Jarvis LA, Rottmann J. and Pogue BW, 2017. Online Combination of EPID & Cherenkov Imaging for 3-D Dosimetry in a Liquid Phantom. IEEE Trans Med Imaging 36:2099–2103. [PubMed: 28644800]

Cala SJ, Kenyon CM, Ferrigno G, Carnevali P, Aliverti A, Pedotti A, Macklem PT and Rochester DF, 1996. Chest wall and lung volume estimation by optical reflectance motion analysis. Journal of applied physiology 81:2680–2689. [PubMed: 9018522]

Carl G, Reitz D, Schonecker S, Pazos M, Freislederer P, Reiner M, Alongi F, Niyazi M, Ganswindt U, Belka C. and Corradini S, 2018. Optical Surface Scanning for Patient Positioning in Radiation Therapy: A Prospective Analysis of 1902 Fractions. Technol Cancer Res Treat 17:1533033818806002.

Catherwood T, McCaughan E, Greer E, Spence RA, McIntosh SA and Winder RJ, 2011. Validation of a passive stereophotogrammetry system for imaging of the breast: a geometric analysis. Med Eng Phys 33:900–905. [PubMed: 21382736]

Cervino LI, Detorie N, Taylor M, Lawson JD, Harry T, Murphy KT, Mundt AJ, Jiang SB and Pawlicki TA, 2012. Initial clinical experience with a frameless and maskless stereotactic radiosurgery treatment. Pract Radiat Oncol 2:54–62. [PubMed: 24674037]

Cervino LI, Gupta S, Rose MA, Yashar C. and Jiang SB, 2009. Using surface imaging and visual coaching to improve the reproducibility and stability of deep-inspiration breath hold for left-breast-cancer radiotherapy. Physics in medicine and biology 54:6853–6865. [PubMed: 19864703]

Cervino LI, Pawlicki T, Lawson JD and Jiang SB, 2010. Frame-less and mask-less cranial stereotactic radiosurgery: a feasibility study. Physics in medicine and biology 55:18631873.

Chang P, Dang J, Dai J. and Sun W, 2021. Real-Time Respiratory Tumor Motion Prediction Based on a Temporal Convolutional Neural Network: Prediction Model Development Study. J Med Internet Res 23:e27235. [PubMed: 34236336]

Cravo Sa A, Fermento A, Neves D, Ferreira S, Silva T, Marques Coelho C, Vaandering A, Roma A, Quaresma S. and Bonnarens E, 2018. Radiotherapy setup displacements in breast cancer patients: 3D surface imaging experience. Reports of practical oncology and radiotherapy : journal of Greatpoland Cancer Center in Poznan and Polish Society of Radiation Oncology 23:61–67. [PubMed: 29379398]

Delombaerde L, Petillion S, Michiels S, Weltens C. and Depuydt T, 2019. Development and accuracy evaluation of a single-camera intra-bore surface scanning system for radiotherapy in an O-ring linac. Phys Imag Radiat Onc 11:21–26.

Delombaerde L, Petillion S, Weltens C. and Depuydt T, 2021. Intra-fraction motion monitoring during fast modulated radiotherapy delivery in a closed-bore gantry linac. Phys Imaging Radiat Oncol 20:51–55. [PubMed: 34765749]

Dickie CI, Parent AL, Chung PW, Catton CN, Craig T, Griffin AM, Panzarella T, Ferguson PC, Wunder JS, Bell RS, Sharpe MB and O’Sullivan B, 2010. Measuring interfractional and intrafractional motion with cone beam computed tomography and an optical localization system for lower extremity soft tissue sarcoma patients treated with preoperative intensity-modulated radiation therapy. Int J Radiat Oncol Biol Phys 78:1437–1444. [PubMed: 20350788]

Djajaputra D. and Li S, 2005. Real-time 3D surface-image-guided beam setup in radiotherapy of breast cancer. Med Phys 32:65–75. [PubMed: 15719956]

Ernst F, Schlaefer A. and Schweikard A, 2011. Predicting the outcome of respiratory motion prediction. Med Phys 38:5569–5581. [PubMed: 21992375]

Fassi A, Seregni M, Riboldi M, Cerveri P, Sarrut D, Ivaldi GB, de Fatis PT, Liotta M. and Baroni G, 2015. Surrogate-driven deformable motion model for organ motion tracking in particle radiation therapy. Physics in medicine and biology 60:1565–1582. [PubMed: 25615399]

Fattori G, Hrbacek J, Regele H, Bula C, Mayor A, Danuser S, Oxley DC, Rechsteiner U, Grossmann M, Via R, Bohlen TT, Bolsi A, Walser M, Togno M, Colvill E, Lempen D, Weber DC, Lomax AJ and Safai S, 2020. Commissioning and Quality Assurance of a novel solution for respiratory-gated PBS proton therapy based on optical tracking of surface markers. Z Med Phys 10.1016/j.zemedi.2020.07.001.

Fattori G, Lomax AJ, Weber DC and Safai S, 2021. Technical assessment of the NDI Polaris Vega optical tracking system. Radiation Oncology 16:87. [PubMed: 33980248]

Fattori G, Safai S, Carmona PF, Peroni M, Perrin R, Weber DC and Lomax AJ, 2017. Monitoring of breathing motion in image-guided PBS proton therapy: comparative analysis of optical and electromagnetic technologies. Radiat Oncol 12:63. [PubMed: 28359341]

Feng SJ, Zuo C, Zhang L, Tao TY, Hu Y, Yin W, Qian JM and Chen Q, 2021. Calibration of fringe projection profilometry: A comparative review. Opt Laser Eng 143.

Freislederer P, Kugele M, Ollers M, Swinnen A, Sauer TO, Bert C, Giantsoudi D, Corradini S. and Batista V, 2020. Recent advanced in Surface Guided Radiation Therapy. Radiat Oncol 15:187. [PubMed: 32736570]

Gierga DP, Riboldi M, Turcotte JC, Sharp GC, Jiang SB, Taghian AG and Chen GT, 2008. Comparison of target registration errors for multiple image-guided techniques in accelerated partial breast irradiation. Int J Radiat Oncol Biol Phys 70:1239–1246. [PubMed: 18207662]

Gierga DP, Turcotte JC, Sharp GC, Sedlacek DE, Cotter CR and Taghian AG, 2012. A voluntary breath-hold treatment technique for the left breast with unfavorable cardiac anatomy using surface imaging. Int J Radiat Oncol Biol Phys 84:e663–668. [PubMed: 22975605]

Gierga DP, Turcotte JC, Tong LW, Chen YL and DeLaney TF, 2014. Analysis of setup uncertainties for extremity sarcoma patients using surface imaging. Pract Radiat Oncol 4:261–266. [PubMed: 25012835]

Glaser AK, Zhang R, Andreozzi JM, Gladstone DJ and Pogue BW, 2015. Cherenkov radiation fluence estimates in tissue for molecular imaging and therapy applications. Physics in medicine and biology 60:6701–6718. [PubMed: 26270125]

Glaser AK, Zhang R, Davis SC, Gladstone DJ and Pogue BW, 2012. Time-gated Cherenkov emission spectroscopy from linear accelerator irradiation of tissue phantoms. Opt Lett 37:1193–1195. [PubMed: 22466192]

Glide-Hurst CK, Ionascu D, Berbeco R. and Yan D, 2011. Coupling surface cameras with on-board fluoroscopy: a feasibility study. Med Phys 38:2937–2947. [PubMed: 21815367]

Gopan O. and Wu Q, 2012. Evaluation of the accuracy of a 3D surface imaging system for patient setup in head and neck cancer radiotherapy. Int J Radiat Oncol Biol Phys 84:547–552. [PubMed: 22365627]

Haraldsson A, Ceberg S, Ceberg C, Back S, Engelholm S. and Engstrom PE, 2020. Surface-guided tomotherapy improves positioning and reduces treatment time: A retrospective analysis of 16 835 treatment fractions. J Appl Clin Med Phys 21:139–148.

Hattel SH, Andersen PA, Wahlstedt IH, Damkjaer S, Saini A. and Thomsen JB, 2019. Evaluation of setup and intrafraction motion for surface guided whole-breast cancer radiotherapy. J Appl Clin Med Phys 20:39–44.

Ho A, Ballangrud A, Li G, Chen Y, Krause K, McCormick B. and Powell SN, 2013. Pneumonitis Rates Following Comprehensive Nodal Irradiation in Breast Cancer Patients: Results of a Phase 1 Feasibility Trial of Intensity Modulated Radiation Therapy. Int J Radiat Oncol Biol Phys 87:S48–S49.

Ho AY, Ballangrud A, Li G, Gupta GP, McCormick B, Gewanter R, Gelblum D, Zinovoy M, Mueller B, Mychalczak B, Dutta P, Borofsky K, Parhar P, Reyngold M, Braunstein LZ, Chawla M, Krause K, Freeman N, Siu CT, Cost Z, Arnold BB, Zhang Z. and Powell SN, 2019. Long-Term Pulmonary Outcomes of a Feasibility Study of Inverse-Planned, Multibeam Intensity Modulated Radiation Therapy in Node-Positive Breast Cancer Patients Receiving Regional Nodal Irradiation. Int J Radiat Oncol Biol Phys 103:1100–1108. [PubMed: 30508620]

Hoisak JD, Paxton A, Waghorn BJ and Pawlicki eds T., 2020. Surface Guided Radiation Therapy. Boca Raton, FL, CRC Press, Taylor & Francis Group.

Hoisak JD, Sixel KE, Tirona R, Cheung PC and Pignol JP, 2006. Prediction of lung tumour position based on spirometry and on abdominal displacement: accuracy and reproducibility. Radiother Oncol 78:339–346. [PubMed: 16537094]

Hoisak JDP and Pawlicki T, 2018. The Role of Optical Surface Imaging Systems in Radiation Therapy. Semin Radiat Oncol 28:185–193. [PubMed: 29933878]

Hughes S, McClelland J, Tarte S, Lawrence D, Ahmad S, Hawkes D. and Landau D, 2009. Assessment of two novel ventilatory surrogates for use in the delivery of gated/tracked radiotherapy for non-small cell lung cancer. Radiother Oncol 91:336–341. [PubMed: 19395076]

Jarvis LA, Hachadorian RL, Jermyn M, Bruza P, Alexander DA, Tendler II, Williams BB, Gladstone DJ, Schaner PE, Zaki BI and Pogue BW, 2021. Initial Clinical Experience of Cherenkov Imaging in External Beam Radiation Therapy Identifies Opportunities to Improve Treatment Delivery. Int J Radiat Oncol Biol Phys 109:1627–1637. [PubMed: 33227443]

Jarvis LA, Zhang R, Gladstone DJ, Jiang S, Hitchcock W, Friedman OD, Glaser AK, Jermyn M. and Pogue BW, 2014. Cherenkov video imaging allows for the first visualization of radiation therapy in real time. Int J Radiat Oncol Biol Phys 89:615–622. [PubMed: 24685442]

Jimenez RB, Batin E, Giantsoudi D, Hazeltine W, Bertolino K, Ho AY, MacDonald SM, Taghian AG and Gierga DP, 2019. Tattoo free setup for partial breast irradiation: A feasibility study. J Appl Clin Med Phys 20:45–50.

Jursinic P, Jordan K. and Chen C, 2022. Positions of radiation isocenter and the couch rotation center established by Winston-Lutz and optical measurements. Tech Innov Patient Support Radiat Oncol 21:46–50. [PubMed: 35243044]

Kai J, Shiomi H, Sasama T, Sato Y, Inoue T, Tamura S. and Inoue T, 1998. Optical highprecision three-dimensional position measurement system suitable for head motion tracking in frameless stereotactic radiosurgery. Comput Aided Surg 3:257–263. [PubMed: 10207650]

Kamath R, Ryken TC, Meeks SL, Pennington EC, Ritchie J. and Buatti JM, 2005. Initial clinical experience with frameless radiosurgery for patients with intracranial metastases. Int J Radiat Oncol Biol Phys 61:1467–1472. [PubMed: 15817352]

Keall PJ, Mageras GS, Balter JM, Emery RS, Forster KM, Jiang SB, Kapatoes JM, Low DA, Murphy MJ, Murray BR, Ramsey CR, Van Herk MB, Vedam SS, Wong JW and Yorke E, 2006. The management of respiratory motion in radiation oncology report of AAPM Task Group 76. Med Phys 33:3874–3900. [PubMed: 17089851]

Kim JI, Chung JH, Kwon O, Min Park J. and Wu HG, 2021. Correlation between 3D scanner image and MRI for tracking volume changes in head and neck cancer patients. J Appl Clin Med Phys 22:86–93. [PubMed: 33522671]

Krengli M, Gaiano S, Mones E, Ballare A, Beldi D, Bolchini C. and Loi G, 2009. Reproducibility of patient setup by surface image registration system in conformal radiotherapy of prostate cancer. Radiat Oncol 4:9. [PubMed: 19232137]

Kuo L, Ballangrud AM, Ho AY, Mechalakos JG, Li G. and Hong L, 2019. A VMAT planning technique for locally advanced breast cancer patients with expander or implant reconstructions requiring comprehensive postmastectomy radiation therapy. Medical dosimetry : official journal of the American Association of Medical Dosimetrists 44:150–154. [PubMed: 29801668]

Laaksomaa M, Sarudis S, Rossi M, Lehtonen T, Pehkonen J, Remes J, Luukkanen H, Skytta T. and Kapanen M, 2019. AlignRT((R)) and Catalyst in whole-breast radiotherapy with DIBH: Is IGRT still needed? J Appl Clin Med Phys 20:97–104.

Lee SK, Huang S, Zhang L, Ballangrud AM, Aristophanous M, Cervino Arriba LI and Li G, 2021. Accuracy of surface-guided patient setup for conventional radiotherapy of brain and nasopharynx cancer. J Appl Clin Med Phys 22:48–57.

Leong B. and Padilla L, 2019. Impact of use of optical surface imaging on initial patient setup for stereotactic body radiotherapy treatments. J Appl Clin Med Phys 20:149–158.

Li G, 2020. Commissioning and routine quality assurance of the VisionRT AlignRT system. In: Surface Guided Radiation Therapy, Hoisak JD, Paxton A, Waghorn BJand Pawlicki T. (J. D. Hoisak, A. Paxton, B. J. Waghorn and T. Pawlicki(J. D. Hoisak, A. Paxton, B. J. Waghorn and T. Pawlickis). CRC Press, Taylor & Francis Group, Boca Raton, pp. 157–186.

Li G, Arora NC, Xie H, Ning H, Lu W, Low D, Citrin D, Kaushal A, Zach L, Camphausen K. and Miller RW, 2009a. Quantitative prediction of respiratory tidal volume based on the external torso volume change: a potential volumetric surrogate. Physics in medicine and biology 54:1963–1978. [PubMed: 19265201]

Li G, Ballangrud A, Chan M, Ma R, Beal K, Yamada Y, Chan T, Lee J, Parhar P, Mechalakos J. and Hunt M, 2015a. Clinical experience with two frameless stereotactic radiosurgery (fSRS) systems using optical surface imaging for motion monitoring. J Appl Clin Med Phys 16:149–162. [PubMed: 26219007]

Li G, Ballangrud A, Kuo LC, Kang H, Kirov A, Lovelock M, Yamada Y, Mechalakos J. and Amols H, 2011a. Motion monitoring for cranial frameless stereotactic radiosurgery using video-based three-dimensional optical surface imaging. Med Phys 38:3981–3994. [PubMed: 21858995]

Li G, Della-Biancia C, Rryn K. and Gil M, 2016a. A novel patient immobilization system to reproduce c-spine curvature for head-and-neck cancer patient in radiotherapy treatment. In: ASTRO. Boston, MA.

Li G, Huang H, Wei J, Li DG, Chen Q, Gaebler CP, Sullivan J, Zatcky J, Rimner A. and Mechalakos J, 2015b. Novel spirometry based on optical surface imaging. Med Phys 42:1690–1697. [PubMed: 25832058]

Li G, Lovelock DM, Mechalakos J, Rao S, Della-Biancia C, Amols H. and Lee N, 2013. Migration from full-head mask to “open-face” mask for immobilization of patients with head and neck cancer. J Appl Clin Med Phys 14:243–254. [PubMed: 24036878]

Li G, Lu W, O’Grady K, Yorke E, Cervino Arriba LI and Hong L, 2021a. A uniform and versatile surface-guided radiotherapy (SGRT) procedure and workflow for high-quality breast DIBH treatment in a multi-center institution. J Appl Clin Med Phys (accepted).

Li G, Mageras GS, Dong L. and Mohan R, 2021b. Image-guided Radiation Therapy. In: Treatment Planning in Radiation Therapy, Khan FM, Sperduto PW. and Gibbons JP (F. M. Khan, Sperduto, P. W. and Gibbons, J. P.)F. M. Khan, Sperduto, P. W. and Gibbons, J. P.s). Wolters Kluwer, pp. 374–403.

Li G, Sun A, Nie X, Moody J, Huang K, Zhang S, Sharma S. and Deasy J, 2018. Introduction of a pseudo demons force to enhance deformation range for robust reconstruction of super-resolution time-resolved 4DMRI. Med Phys 45:5197–5207. [PubMed: 30203474]

Li G, Wei J, Huang H, Chen Q, Gaebler CP, Lin T, Yuan A, Rimner A. and Mechalakos J, 2016b. Characterization of optical-surface-imaging-based spirometry for respiratory surrogating in radiotherapy. Med Phys 43:1348–1360. [PubMed: 26936719]

Li G, Wei J, Huang H, Gaebler CP, Yuan A. and Deasy JO, 2015c. Automatic assessment of average diaphragm motion trajectory from 4DCT images through machine learning. Biomed Phys Eng Express 1:045015. [PubMed: 27110388]

Li G, Wei J, Kadbi M, Moody J, Sun A, Zhang S, Markova S, Zakian K, Hunt M. and Deasy JO, 2017. Novel Super-Resolution Approach to Time-Resolved Volumetric 4-Dimensional Magnetic Resonance Imaging With High Spatiotemporal Resolution for Multi-Breathing Cycle Motion Assessment. Int J Radiat Oncol Biol Phys 98:454–462. [PubMed: 28463165]

Li G, Xie H, Ning H, Lu W, Low D, Citrin D, Kaushal A, Zach L, Camphausen K. and Miller RW, 2009b. A novel analytical approach to the prediction of respiratory diaphragm motion based on external torso volume change. Physics in medicine and biology 54:41134130.

Li G, Yamada Y. and Ballangrud A, 2020. Image Guidance for Frameless Radiosurgery Including Surface Mapping - A Case-Based Approach. In: Radiotherapy in Managing Brain Metastases, Yamada Y, Chang E, Fiveash J. and Knisely J. (Y. Yamada, E. Chang, J. Fiveash and J. Knisely(Y. Yamada, E. Chang, J. Fiveash and J. Kniselys). Springer, Switzerland, pp. 311–322.

Li R, Lewis JH, Jia X, Zhao T, Liu W, Wuenschel S, Lamb J, Yang D, Low DA and Jiang SB, 2011b. On a PCA-based lung motion model. Physics in medicine and biology 56:6009–6030. [PubMed: 21865624]

Li S, DeWeese T, Movsas B, Liu D, Frassica D, Kim J, Chen Q. and Walker E, 2012. Initial validation and clinical experience with 3D optical-surface-guided whole breast irradiation of breast cancer. Technol Cancer Res Treat 11:57–68. [PubMed: 22181332]

Low DA, Parikh PJ, Lu W, Dempsey JF, Wahab SH, Hubenschmidt JP, Nystrom MM, Handoko M. and Bradley JD, 2005. Novel breathing motion model for radiotherapy. Int J Radiat Oncol Biol Phys 63:921–929. [PubMed: 16140468]

Lyatskaya Y, James S, Killoran JH, Soto R, Mamon HJ, Chin L. and Allen AM, 2008. Infrared-guided patient setup for lung cancer patients. Int J Radiat Oncol Biol Phys 71:1124–1133. [PubMed: 18249503]

Mageras GS and Yorke E, 2004. Deep inspiration breath hold and respiratory gating strategies for reducing organ motion in radiation treatment. Semin Radiat Oncol 14:65–75. [PubMed: 14752734]

Mah D, Hanley J, Rosenzweig KE, Yorke E, Braban L, Ling CC, Leibel SA and Mageras G, 2000. Technical aspects of the deep inspiration breath-hold technique in the treatment of thoracic cancer. Int J Radiat Oncol Biol Phys 48:1175–1185. [PubMed: 11072177]

Mannerberg A, Kugele M, Hamid S, Edvardsson A, Petersson K, Gunnlaugsson A, Back SAJ, Engelholm S. and Ceberg S, 2021. Faster and more accurate patient positioning with surface guided radiotherapy for ultra-hypofractionated prostate cancer patients. Tech Innov Patient Support Radiat Oncol 19:41–45. [PubMed: 34527818]

Meeks SL, Tome WA, Willoughby TR, Kupelian PA, Wagner TH, Buatti JM and Bova FJ, 2005. Optically guided patient positioning techniques. Semin Radiat Oncol 15:192–201. [PubMed: 15983944]

Meyer J, Smith W, Geneser S, Koger B, Kalet AM, Young LA, Cao N, Price RG, Norris C, Horton T, Womeldorf J, Alexandrian AN and Wootton LS, 2020. Characterizing a deformable registration algorithm for surface-guided breast radiotherapy. Med Phys 47:352–362. [PubMed: 31724177]

Milewski AR, Olek D, Deasy JO, Rimner A. and Li G, 2019. Enhancement of Long-Term External-Internal Correlation by Phase-Shift Detection and Correction Based on Concurrent External Bellows and Internal Navigator Signals. Adv Radiat Oncol 4:377–389. [PubMed: 31011684]

Naumann P, Batista V, Farnia B, Fischer J, Liermann J, Tonndorf-Martini E, Rhein B. and Debus J, 2020. Feasibility of Optical Surface-Guidance for Position Verification and Monitoring of Stereotactic Body Radiotherapy in Deep-Inspiration Breath-Hold. Frontiers in oncology 10:573279. [PubMed: 33102232]

Nguyen D, Farah J, Barbet N. and Khodri M, 2020. Commissioning and performance testing of the first prototype of AlignRT InBore a Halcyon and Ethos-dedicated surface guided radiation therapy platform. Phys Med 80:159–166. [PubMed: 33189046]

Nie X, Saleh Z, Kadbi M, Zakian K, Deasy J, Rimner A. and Li G, 2020. A super-resolution framework for the reconstruction of T2-weighted (T2w) time-resolved (TR) 4DMRI 1285 using T1w TR-4DMRI as the guidance. Med Phys 47:3091–3102. [PubMed: 32166757]

O’Connell RL, Stevens RJ, Harris PA and Rusby JE, 2015. Review of three-dimensional (3D) surface imaging for oncoplastic, reconstructive and aesthetic breast surgery. Breast 24:331–342. [PubMed: 25935829]

Olesen OV, Paulsen RR, Hojgaard L, Roed B. and Larsen R, 2012. Motion tracking for medical imaging: a nonvisible structured light tracking approach. IEEE Trans Med Imaging 31:79–87. [PubMed: 21859614]

Padilla L, Havnen-Smith A, Cervino L. and Al-Hallaq HA, 2019. A survey of surface imaging use in radiation oncology in the United States. J Appl Clin Med Phys 20:70–77.

Padilla L, Pearson EA and Pelizzari CA, 2015. Collision prediction software for radiotherapy treatments. Med Phys 42:6448–6456. [PubMed: 26520734]

Paxton AB, Manger RP, Pawlicki T. and Kim GY, 2017. Evaluation of a surface imaging system’s isocenter calibration methods. J Appl Clin Med Phys 18:85–91. [PubMed: 28300386]

Pazos M, Fiorentino A, Gaasch A, Schonecker S, Reitz D, Heinz C, Niyazi M, Duma MN, Alongi F, Belka C. and Corradini S, 2019. Dose variability in different lymph node levels during locoregional breast cancer irradiation: the impact of deep-inspiration breath hold. Strahlenther Onkol 195:13–20. [PubMed: 30143814]

Peng JL, Kahler D, Li JG, Amdur RJ, Vanek KN and Liu C, 2011. Feasibility study of performing IGRT system daily QA using a commercial QA device. J Appl Clin Med Phys 12:3535. [PubMed: 21844867]

Placht S, Stancanello J, Schaller C, Balda M. and Angelopoulou E, 2012. Fast time-of-flight camera based surface registration for radiotherapy patient positioning. Med Phys 39:4–17. [PubMed: 22225270]

Price GJ, Parkhurst JM, Sharrock PJ and Moore CJ, 2012. Real-time optical measurement of the dynamic body surface for use in guided radiotherapy. Physics in medicine and biology 57:415–436. [PubMed: 22173038]

Riboldi M, Baroni G, Spadea MF, Bassanini F, Tagaste B, Garibaldi C, Orecchia R. and Pedotti A, 2006. Robust frameless stereotactic localization in extra-cranial radiotherapy. Med Phys 33:1141–1152. [PubMed: 16696492]

Riboldi M, Gierga DP, Chen GT and Baroni G, 2009. Accuracy in breast shape alignment with 3D surface fitting algorithms. Med Phys 36:1193–1198. [PubMed: 19472625]

Rigley J, Robertson P. and Scattergood L, 2020. Radiotherapy without tattoos: Could this work? Radiography (Lond) 26:288–293. [PubMed: 32245712]

Schoffel PJ, Harms W, Sroka-Perez G, Schlegel W. and Karger CP, 2007. Accuracy of a commercial optical 3D surface imaging system for realignment of patients for radiotherapy of the thorax. Physics in medicine and biology 52:3949–3963. [PubMed: 17664587]

Sharma M, Dos Santos T, Papanikolopoulos NP and Hui SK, 2011. Feasibility of intrafraction whole-body motion tracking for total marrow irradiation. Journal of biomedical optics 16:058002. [PubMed: 21639586]

Shi C, Tang X. and Chan M, 2017. Evaluation of the new respiratory gating system. Precis Radiat Oncol 1:127–133. [PubMed: 29722356]

Silverstein E. and Snyder M, 2017. Implementation of facial recognition with Microsoft Kinect v2 sensor for patient verification. Med Phys 44:2391–2399. [PubMed: 28370061]

Song Y, Zhai X, Liang Y, Zeng C, Mueller B. and Li G, 2022. Evidence-based definition of region of interest (ROI) for abdominal DIBH surface-guided radiotherapy. ASTRO Annual Meeting.

Spadea MF, Baroni G, Riboldi M, Tagaste B, Garibaldi C, Orecchia R. and Pedotti A, 2006. Patient set-up verification by infrared optical localization and body surface sensing in breast radiation therapy. Radiother Oncol 79:170–178. [PubMed: 16574263]

Swinnen ACC, Ollers MC, Loon Ong C. and Verhaegen F, 2020. The potential of an optical surface tracking system in non-coplanar single isocenter treatments of multiple brain metastases. J Appl Clin Med Phys 21:63–72. [PubMed: 32237274]

Tang X, Zagar TM, Bair E, Jones EL, Fried D, Zhang L, Tracton G, Xu Z, Leach T, Chang S. and Marks LB, 2014. Clinical experience with 3-dimensional surface matching-based deep inspiration breath hold for left-sided breast cancer radiation therapy. Pract Radiat Oncol 4:e151–e158. [PubMed: 24766689]

Tanguturi SK, Lyatskaya Y, Chen Y, Catalano PJ, Chen MH, Yeo WP, Marques A, Truong L, Yeh M, Orlina L, Wong JS, Punglia RS and Bellon JR, 2015. Prospective assessment of deep inspiration breath-hold using 3-dimensional surface tracking for irradiation of left-sided breast cancer. Pract Radiat Oncol 5:358–365. [PubMed: 26231594]

Theodoulou M. and Seidman AD, 2003. Cardiac effects of adjuvant therapy for early breast cancer. Seminars in oncology 30:730–739. [PubMed: 14663774]

Waghorn BJ, 2020. Technical Overview and Features of the VIsion RT AlignRT System. In: Surface Guided Radiation Therapy, Hoisak JD, Paxton A, Waghorn BJ and Pawlicki T. (J. D. Hoisak, A. Paxton, B. J. Waghorn and T. Pawlicki(J. D. Hoisak, A. Paxton, B. J. Waghorn and T. Pawlickis). CRC Press, Taylor & Francis Group, Boca Raton, FL, pp. 95–116.

Wagner B, Stuber P, Wissel T, Bruder R, Schweikard A. and Ernst F, 2014. Accuracy analysis for triangulation and tracking based on time-multiplexed structured light. Med Phys 41:082701. [PubMed: 25086557]

Wang X, Ma C, Davis R, Parikh RR, Jabbour SK, Haffty BG, Yue NJ, Nie K. and Zhang Y, 2019. A novel approach to Verify air gap and SSD for proton radiotherapy using surface imaging. Radiat Oncol 14:224. [PubMed: 31829246]

Wei W, Ioannides PJ, Sehgal V. and Daroui P, 2020. Quantifying the impact of optical surface guidance in the treatment of cancers of the head and neck. J Appl Clin Med Phys 21:73–82.

Wentz T, Fayad H, Bert J, Pradier O, Clement JF, Vourch S, Boussion N. and Visvikis D, 2012. Accuracy of dynamic patient surface monitoring using a time-of-flight camera and B-spline modeling for respiratory motion characterization. Physics in medicine and biology 57:4175–4193. [PubMed: 22684018]

Werner R, White B, Handels H, Lu W. and Low DA, 2010. Technical note: development of a tidal volume surrogate that replaces spirometry for physiological breathing monitoring in 4D CT. Med Phys 37:615–619. [PubMed: 20229870]

Wiant D, Wentworth S, Liu H. and Sintay B, 2015. How Important Is a Reproducible Breath Hold for Deep Inspiration Breath Hold Breast Radiation Therapy? Int J Radiat Oncol Biol Phys 93:901–907. [PubMed: 26530760]

Wiersma RD, McCabe BP, Belcher AH, Jensen PJ, Smith B. and Aydogan B, 2016. Technical Note: High temporal resolution characterization of gating response time. Med Phys 43:2802–2806. [PubMed: 27277028]

Wikstrom KA, Isacsson UM, Nilsson KM and Ahnesjo A, 2021. Evaluation of four surface surrogates for modeling lung tumor positions over several fractions in radiotherapy. J Appl Clin Med Phys 22:103–112.

Willoughby T, Lehmann J, Bencomo JA, Jani SK, Santanam L, Sethi A, Solberg TD, Tome WA and Waldron TJ, 2012. Quality assurance for nonradiographic radiotherapy localization and positioning systems: report of Task Group 147. Med Phys 39:1728–1747. [PubMed: 22482598]

Winder J, McRitchie I, McKnight W. and Cooke S, 2005. Virtual surgical planning and CAD/CAM in the treatment of cranial defects. Studies in health technology and informatics 111:599–601. [PubMed: 15718805]

Yang TJ, Tao R, Elkhuizen PH, van Vliet-Vroegindeweij C, Li G. and Powell SN, 2013. Tumor bed delineation for external beam accelerated partial breast irradiation: a systematic review. Radiother Oncol 108:181–189. [PubMed: 23806188]

Yuan A, Wei J, Gaebler CP, Huang H, Olek D. and Li G, 2016. A Novel Respiratory Motion Perturbation Model Adaptable to Patient Breathing Irregularities. Int J Radiat Oncol Biol Phys 96:1087–1096. [PubMed: 27745981]

Zhang L, Vijayan S, Huang S, Song Y, Li T, Li X, Hipp E, Chan MF, Kuo HC, Tang X, Tang G, Lim SB, Lovelock DM, Ballangrud A. and Li G, 2021. Commissioning of optical surface imaging systems for cranial frameless stereotactic radiosurgery. J Appl Clin Med Phys 22:182–190. [PubMed: 33779052]

Zhang Q, Pevsner A, Hertanto A, Hu YC, Rosenzweig KE, Ling CC and Mageras GS, 2007. A patient-specific respiratory model of anatomical motion for radiation treatment planning. Med Phys 34:4772–4781. [PubMed: 18196805]

Zhao H, Wang B, Sarkar V, Rassiah-Szegedi P, Huang YJ, Szegedi M, Huang L, Gonzalez V. and Salter B, 2016. Comparison of surface matching and target matching for image-guided pelvic radiation therapy for both supine and prone patient positions. J Appl Clin Med Phys 17:14–24.

Zhao H, Williams N, Poppe M, Sarkar V, Wang B, Rassiah-Szegedi P, Huang YJ, Kokeny K, Gaffney D. and Salter B, 2019. Comparison of surface guidance and target matching for image-guided accelerated partial breast irradiation (APBI). Med Phys 46:4717–4724. [PubMed: 31509632]

Zhou S, Li J, Du Y, Yu S, Wang M, Wu H. and Yue H, 2021. Development and Longitudinal Analysis of Plan-Based Streamlined Quality Assurance on Multiple Positioning Guidance Systems With Single Phantom Setup. Frontiers in oncology 11:683733.

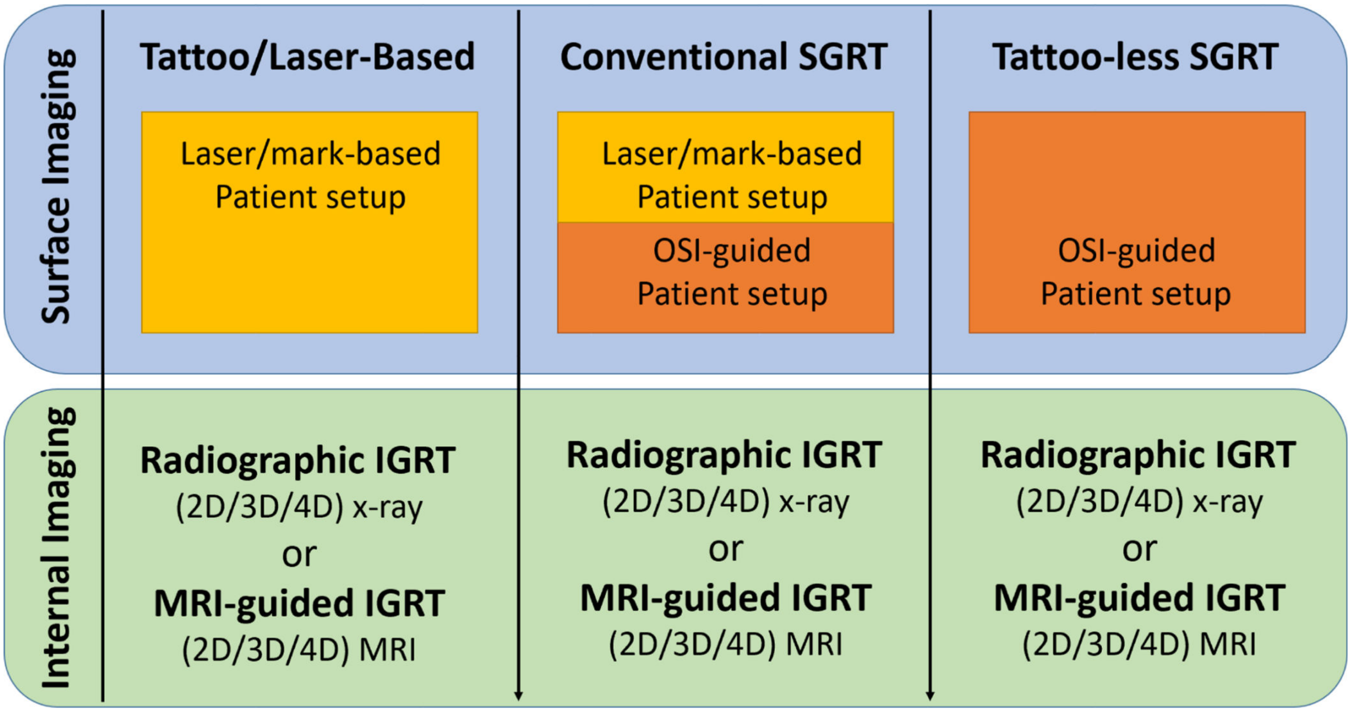

Figure 1.

Illustration of the differences among tattoo/laser-based, conventional SGRT, and tattoo-less SGRT procedures for patient setup, in which either radiographic or MR-guided IGRT should be prescribed for all hypo-fractional stereotactic body radiotherapy (SBRT) but may not be necessary for conventional 3D radiotherapy treatments. The clinical workflow is from the top (SGRT) to the bottom (IGRT). In the conventional SGRT procedure, the laser/mark is still used for initial patient alignment, whereas the tattoo-less SGRT is the first alignment for patient setup.

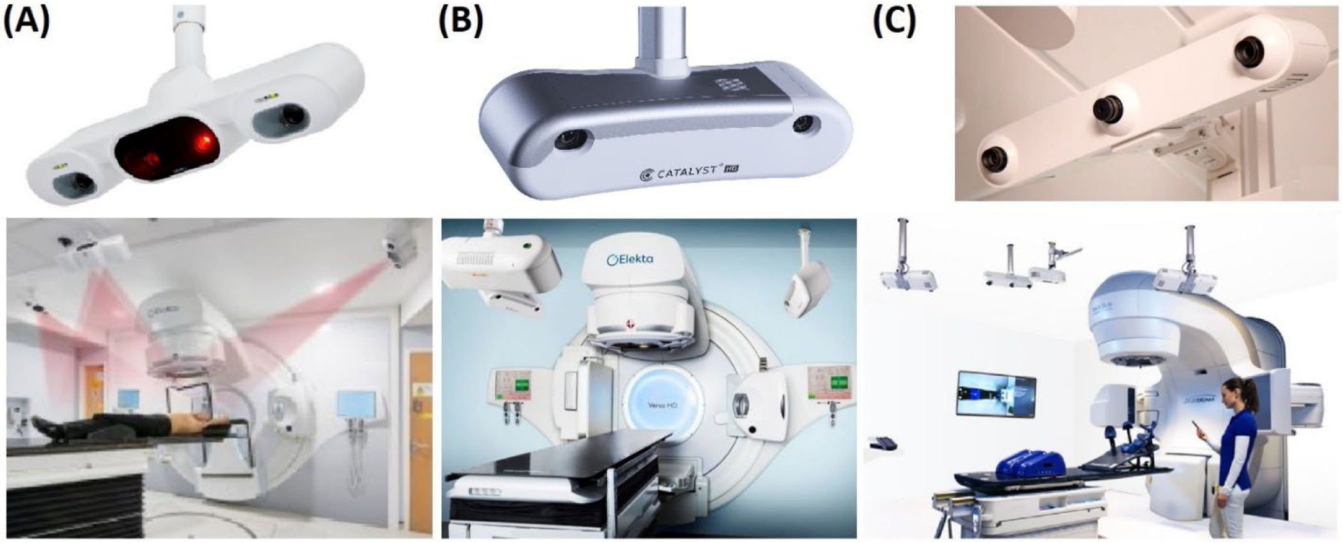

Figure 2.

Three major commercial OSI systems are used for SGRT applications in radiotherapy clinics. (A) AlignRT Advanced system, (B) Catalyst+ HD system, and (C) IDENTIFY system. The top row shows the cameras (and projector) in the pod and the bottom row shows the 3-pod OSI systems installed in the treatment room. Note that Varian's IDENTIFY system has a 4th TOF camera pod above the couch. (Images are taken from vendors' websites with permission, courtesy of these vendors, copyright (2022), and all rights reserved)

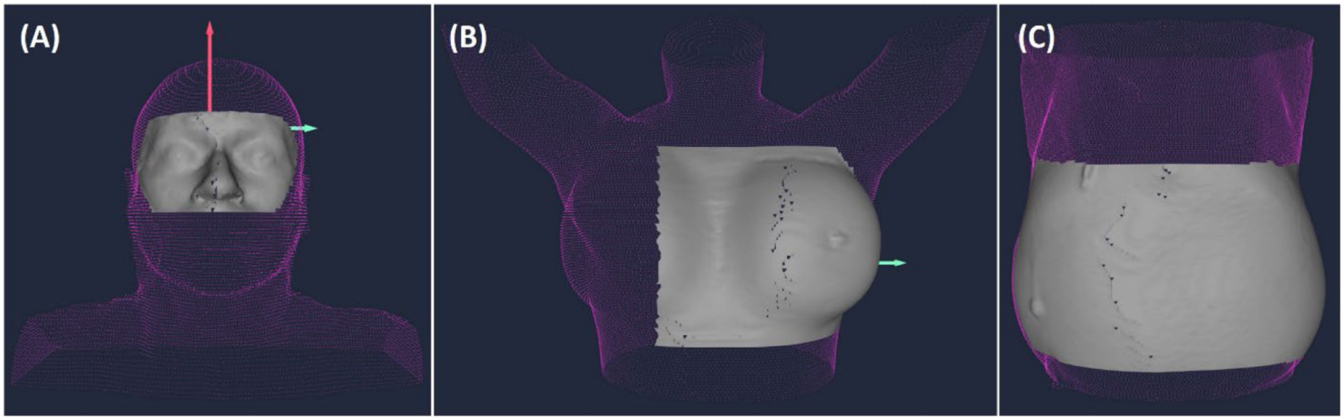

Figure 3.

Three examples of regions of interest (ROIs) for SGRT setup and motion monitoring to treat (A) brain, (B) breast, and (C) abdominal cancer. The reference surface is presented in mesh (pink) from the simulation CT and the ROI is shown as a solid surface (white). Note that the breast CT covers part of the arm and chin to allow their alignment before the breast setup.

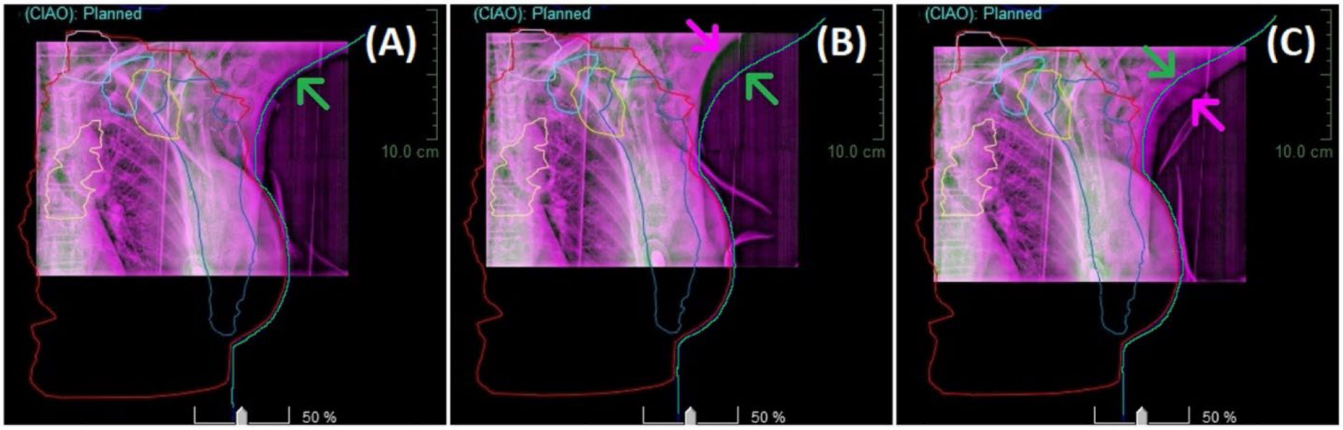

Figure 4.

Three examples of radiographic images (pink) fusion with simulation CT (green body contour) of a locally advanced breast implant in 3 fractions of volumetric-modulated arc therapy (VMAT) treatments to a large planning tumor volume (PTV: red). The green arrows point to an ideal arm setup (A), medial arm setup (B), and lateral arm setup (C), despite the breast ROI being well aligned in all cases (simulation body position: green). The 2 different arm positions (B and C) will lead to displacements of the local lymph nodes away from their simulation positions, including the axillary nodes: level I (blue), II (yellow), and III (light blue), super clavicle node (grey), and internal mammary node (badge). The 2DkV image has a limited FOV, so the inferior breast image is not shown. (Image from Li, et al. 2021a with permission)

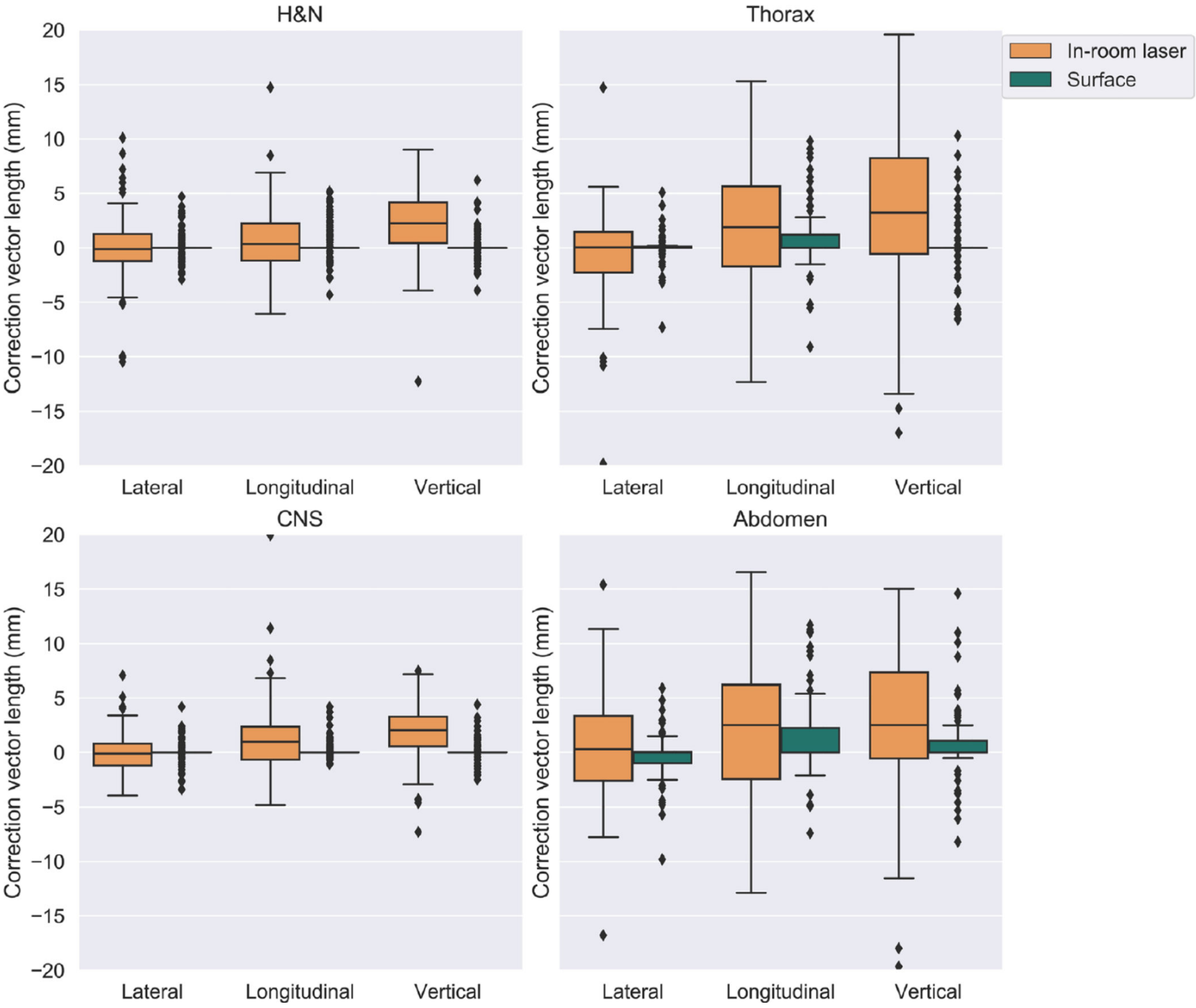

Figure 5.

Demonstration of residual setup uncertainties and error ranges in three translational directions between tattoo/laser-based and OSI-based patient setups, using MVCT (Megavoltage CT) as the reference (Haraldsson, et al. 2020). The differences are significant ($p<0.005$) for all 4 anatomical sites. Although the mean errors are small, the error ranges are large. (images are 745 taken from Haraldsson, et al. 2020 with permission)

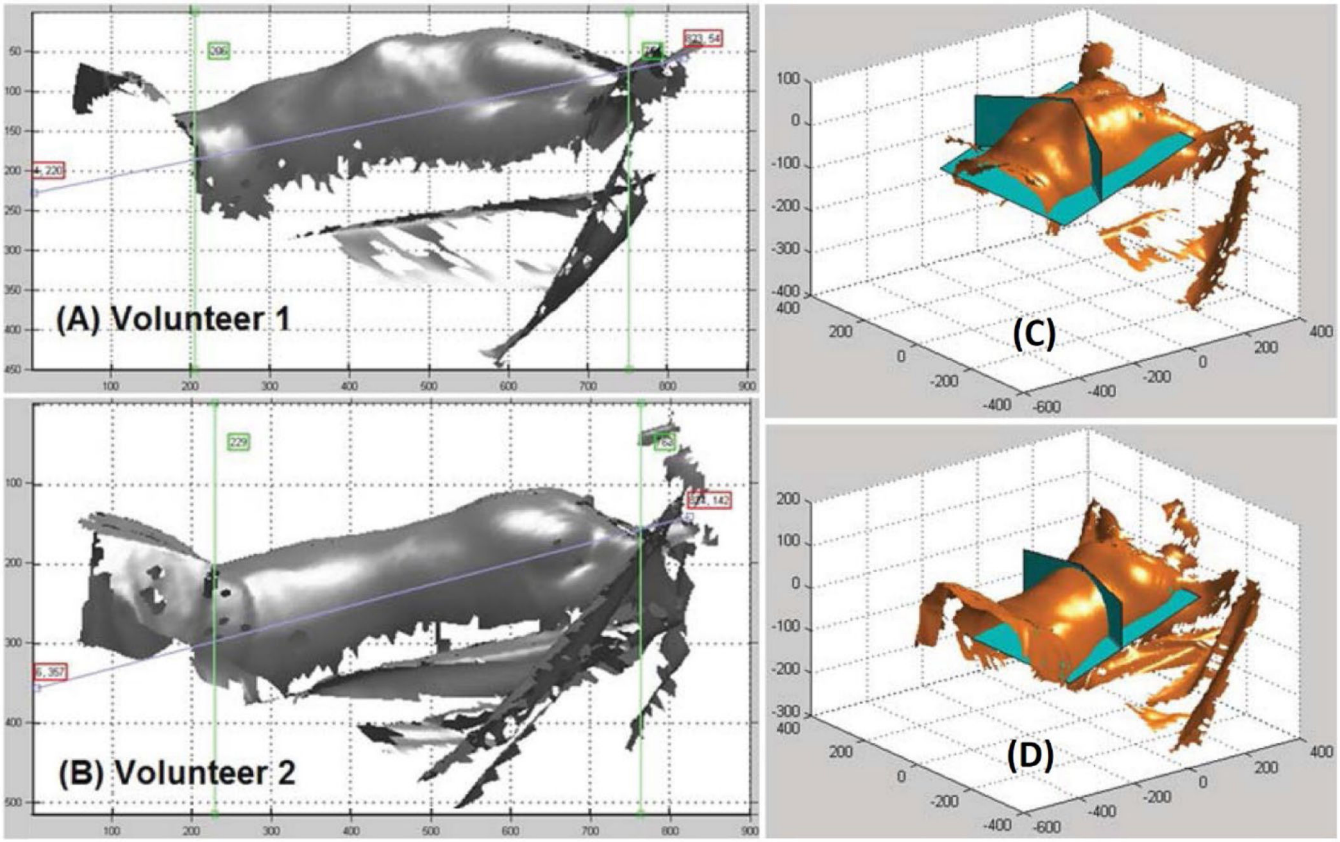

Figure 6.

Illustration of AlignRT torso surface images of a male (A and C) and a female subject (B and D) acquired using the AlignRT system. The volume of interest is defined between the 2 vertical lines (green), tilted horizontal line (purple), and anterior surface (A and B). Using the full-exhalation torso surface image as the reference, the torso volume changes are calculated for OSI-based spirometry. The 3D surface views are shown in (C and D) with 3 cutting planes: the tiled horizontal plane, and the 2 vertical planes along the edge of the rib cage to separate the thoracic and abdominal motions. The images are taken from the references (Li, et al. 2015b; Li, et al. 2016b) with permission.

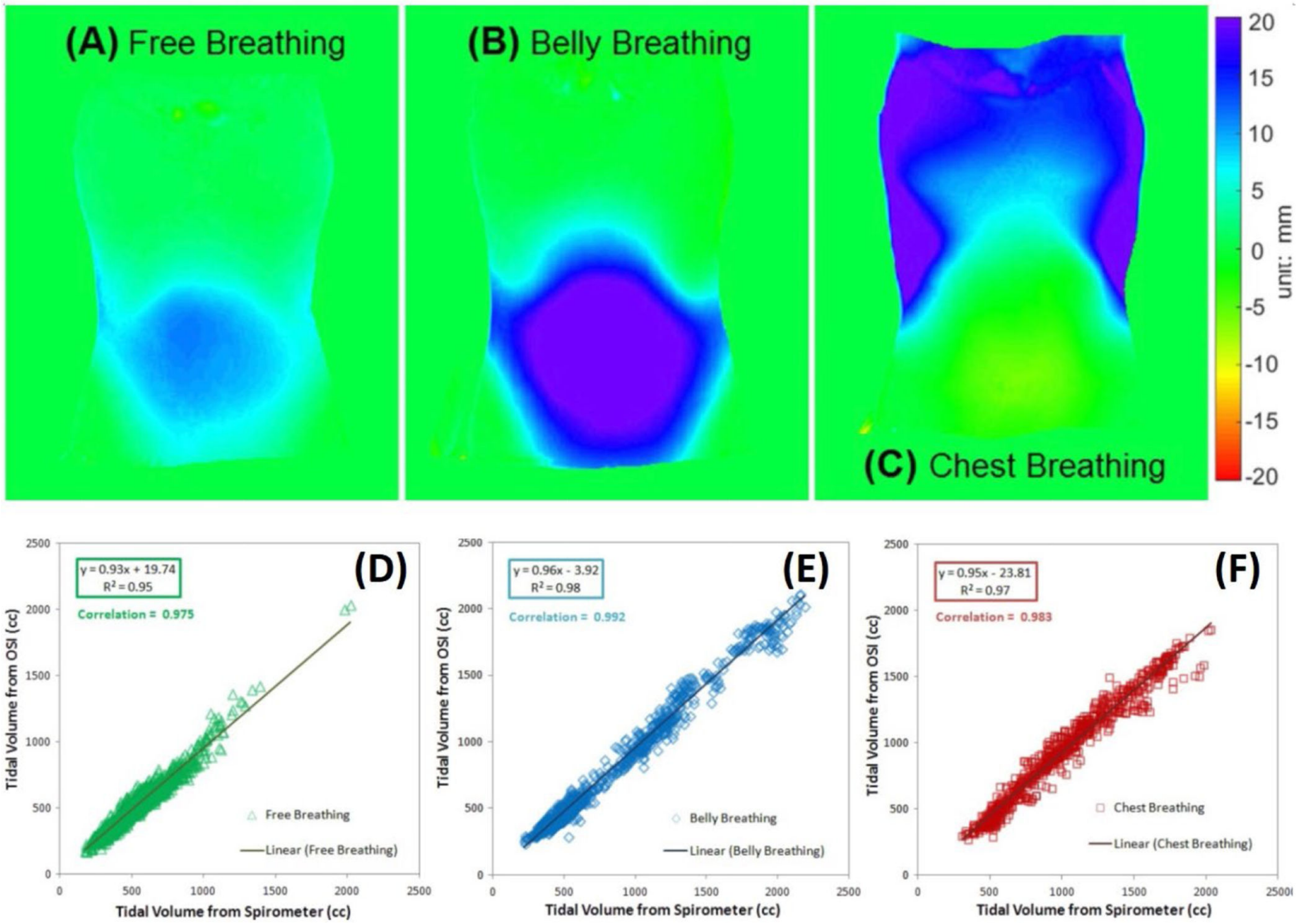

Figure 7.

Illustration of 3 different breathing patterns: (A) free-breathing, (B) belly breathing, and (C) chest breathing, and the consistency between OSI-based and conventional spirometry measurements in 11 volunteers with 78±28 breathing cycles per subject on average in FB (D), and about half of breathing cycles in belly breathing (E) and chest breathing (F). The linear fit and correlation coefficient are shown. Images are taken from (Li, et al. 2016b) with permission.